
BWR Full Integral Simulation Test (FIST) Program TRAC-BWR Model Development Volume 3 — Developmental Assessment for Plant Application

Prepared by Y. K. Cheung, J. G. M. Andersen, K. H. Chu, J. C. Shaug

Nuclear Technology and Fuel Division
General Electric Company

Prepared for
U.S. Nuclear Regulatory Commission

and
Electric Power Research Institute

and
General Electric Company

NOTICE

This report was prepared as an account of work sponsored by an agency of the United States Government. Neither the United States Government nor any agency thereof, or any of their employees, makes any warranty, expressed or implied, or assumes any legal liability of responsibility for any third party's use, or the results of such use, of any information, apparatus, product or process disclosed in this report, or represents that its use by such third party would not infringe privately owned rights.

NOTICE

Availability of Reference Materials Cited in NRC Publications

Most documents cited in NRC publications will be available from one of the following sources:

1. The NRC Public Document Room, 1717 H Street, N.W.
Washington, DC 20555
2. The Superintendent of Documents, U.S. Government Printing Office, Post Office Box 37082,
Washington, DC 20013-7082
3. The National Technical Information Service, Springfield, VA 22161

Although the listing that follows represents the majority of documents cited in NRC publications, it is not intended to be exhaustive.

Referenced documents available for inspection and copying for a fee from the NRC Public Document Room include NRC correspondence and internal NRC memoranda; NRC Office of Inspection and Enforcement bulletins, circulars, information notices, inspection and investigation notices; Licensee Event Reports; vendor reports and correspondence; Commission papers; and applicant and licensee documents and correspondence.

The following documents in the NUREG series are available for purchase from the GPO Sales Program: formal NRC staff and contractor reports, NRC-sponsored conference proceedings, and NRC booklets and brochures. Also available are Regulatory Guides, NRC regulations in the *Code of Federal Regulations*, and *Nuclear Regulatory Commission Issuances*.

Documents available from the National Technical Information Service include NUREG series reports and technical reports prepared by other federal agencies and reports prepared by the Atomic Energy Commission, forerunner agency to the Nuclear Regulatory Commission.

Documents available from public and special technical libraries include all open literature items, such as books, journal and periodical articles, and transactions. *Federal Register* notices, federal and state legislation, and congressional reports can usually be obtained from these libraries.

Documents such as theses, dissertations, foreign reports and translations, and non-NRC conference proceedings are available for purchase from the organization sponsoring the publication cited.

Single copies of NRC draft reports are available free, to the extent of supply, upon written request to the Division of Technical Information and Document Control, U.S. Nuclear Regulatory Commission, Washington, DC 20555.

Copies of industry codes and standards used in a substantive manner in the NRC regulatory process are maintained at the NRC Library, 7920 Norfolk Avenue, Bethesda, Maryland, and are available there for reference use by the public. Codes and standards are usually copyrighted and may be purchased from the originating organization or, if they are American National Standards, from the American National Standards Institute, 1430 Broadway, New York, NY 10018.

BWR Full Integral Simulation Test (FIST) Program TRAC-BWR Model Development Volume 3 — Developmental Assessment for Plant Application

Manuscript Completed: June 1985
Date Published: November 1985

Prepared by
Y. K. Cheung, J. G. M. Andersen, K. H. Chu, J. C. Shaug

Nuclear Technology and Fuel Division
General Electric Company
San Jose, CA 95125

Prepared for
Division of Accident Evaluation
Office of Nuclear Regulatory Research
U.S. Nuclear Regulatory Commission
Washington, D.C. 20555
NRC FIN No. B3014

and
Electric Power Research Institute
3412 Hillview Avenue
Palo Alto, CA 94303

and
Nuclear Technology and Fuel Division
General Electric Company
San Jose, CA 95125

PREVIOUS REPORTS IN BWR FIST SERIES

BWR Full Integral Simulation Test (FIST) Program Test Plan, J. E. Thompson, General Electric Company, NUREG/CR-2575, September 1983.

BWR Full Integral Simulation Test (FIST) Program Facility Description Report, A. G. Stephens, General Electric Company, NUREG/CR-2576, September 1984.

BWR Full Integral Simulation Test (FIST) Phase I Test Results, W. S. Hwang, Md. Alamgir, W. A. Sutherland, General Electric Company, NUREG/CR-3711, September 1984.

BWR Full Integral Simulation Test (FIST) Program: TRAC-BWR Model Development, Volume 1-Numerical Methods, J. G. M. Andersen, C. L. Heck, General Electric Company, NUREC/CR-4127-1, October 1985.

BWR Full Integral Simulation Test (FIST) Program: TRAC-BWR Model Development, Volume 2-Models, K. H. Chu, J. G. M. Andersen, Y. K. Cheung, J. C. Shaug, General Electric Company, NUREC/CR-4127-2, October 1985.

NUREG/CR-4127-3
EPRI NP-3987-3
GEAP-30875-3
June 1985

BWR FULL INTEGRAL SIMULATION TEST (FIST) PROGRAM

CONTRACT NRC-04-76-215

TRAC-BWR MODEL DEVELOPMENT

VOLUME 3 - DEVELOPMENTAL ASSESSMENT FOR PLANT APPLICATION

Y. K. Cheung

J. G. M. Andersen

K. H. Chu

J. C. Shaug

Approved: *B. S. Shiralkar*
B. S. Shiralkar, Manager
Transient Methods

Approved: *L. L. Myers*
L. L. Myers, Program Manager
External Programs

Approved: *G. E. Dix*
G. E. Dix, Manager
Core Methods

Approved: *J. E. Wood*
J. E. Wood, Manager
Core and Fuel Technology

NUCLEAR ENERGY BUSINESS OPERATIONS • GENERAL ELECTRIC COMPANY
SAN JOSE, CALIFORNIA 95125

GENERAL  ELECTRIC

ABSTRACT

The TRACB04 computer code has been developed under the model development tasks in the FIST Program. This report describes two developmental assessment calculations performed on BWR plants with TRACB04. A BWR/2 Design Basis Accident (DBA) including the containment response and a BWR/4 DBA with Low Pressure Coolant Injection (LPCI) water injected into the lower plenum were calculated and results of these cases were documented. These cases serve to test some of the new features of the TRACB04 (air field, containment model, "water packing" fixes and faster numerics in the three dimensional vessel component) and to demonstrate that the code has been assembled properly. They also provide best estimate LOCA results for the two plant types.

TABLE OF CONTENTS

<u>Section</u>	<u>Page</u>
1. INTRODUCTION	1-1
2. BWR/2 RECIRCULATION LINE BREAK	2-1
2.1 Objectives of BWR/2 DBA Calculation	2-1
2.2 Case Descriptions	2-1
2.3 Results	2-6
2.4 Main Observations	2-27
3. BWR/4 RECIRCULATION LINE BREAK	3-1
3.1 Objective of BWR/4 DBA Calculation	3-1
3.2 Case Descriptions	3-1
3.3 Results	3-6
3.4 Main Observations	3-32
4. RUN-TIME STATISTICS	4-1
5. CONCLUSION	5-1
6. REFERENCES	6-1

TABLES

<u>Table</u>		<u>Page</u>
2-1	BWR/2 DBA Calculation - Assumptions	2-3
2-2	BWR/2 DBA Calculation - Initial Conditions	2-4
2-3	Sequence of Events for BWR/2 DBA	2-9
3-1	BWR/4 DBA Calculation - Assumptions	3-2
3-2	BWR/4 DBA Calculation - Initial Conditions	3-4
3-3	Sequence of Events for BWR/4 DBA	3-8
4-1	Run-time Statistics for the BWR/2 and BWR/4 DBA Calculations with TRACB04	4-2
4-2	Summary of Run-time Statistics for the BWR/6 DBA Calculations with TRACB02, TRACB03 and TRACB04	4-3

ILLUSTRATIONS

<u>Figure</u>		<u>Page</u>
1-1	Major Milestone in TRAC-BWR Development	1-2
2-1	TRACB04 Nodalization of BWR/2 Reactor Assembly	2-5
2-2	Schematic of TRACB04 Nodalization of BWR/2 Vessel and Containment	2-7
2-3	BWR/2 DBA Steam Dome Pressure	2-11
2-4	BWR/2 DBA Break Flow from the Recirculation Pump Side	2-12
2-5a	BWR/2 DBA Break Flow from the Vessel Side	2-13
2-5b	BWR/2 DBA Break Flow from the Vessel Side (Blow-up Scale)	2-14
2-6	BWR/2 DBA Mass Flow at SEO of Low Power CHAN (76 Bundles)	2-15
2-7	BWR/2 DBA Mass Flow at Top of Low Power CHAN (76 Bundles)	2-16
2-8	BWR/2 DBA Mass Flow at SEO of Average Power CHAN (424 Bundles)	2-17
2-9	BWR/2 DBA Mass Flow at Top of Average Power CHAN (424 Bundles)	2-18
2-10	BWR/2 DBA Mass Flow at SEO of High Power CHAN #1 (24 Bundles)	2-19
2-11	BWR/2 DBA Mass Flow at Top of High Power CHAN #1 (24 Bundles)	2-20
2-12	BWR/2 DBA Mass Flow at SEO of High Power CHAN #2 (36 Bundles)	2-21
2-13	BWR/2 DBA Mass Flow at Top of High Power CHAN #2 (36 Bundles)	2-22
2-14	BWR/2 DBA Partial Air Pressures at Bottom Level of Upper Plenum	2-24
2-15	BWR/2 DBA Total and Partial Air Pressures in Cell 1 at Bottom Level of Upper Plenum	2-25
2-16	BWR/2 DBA Water Subcooling in Cell 1 at Bottom Level of Upper Plenum	2-26
2-17	BWR/2 DBA Peak Cladding Temperature in Low Power Bundle	2-28
2-18	BWR/2 DBA Peak Cladding Temperature in Average Power Bundle	2-29
2-19	BWR/2 DBA Peak Cladding Temperature in High Power Bundle (CHAN #1)	2-30
2-20	BWR/2 DBA Peak Cladding Temperature in High Power Bundle (CHAN #2)	2-31
2-21	BWR/2 DBA Total and Partial Air Pressure in the Drywell	2-32
2-22	BWR/2 DBA Liquid Mass Inventory in the Drywell	2-33

ILLUSTRATIONS (Continued)

<u>Figure</u>		<u>Page</u>
2-23	BWR/2 DBA Total and Partial Air Pressure in the Wetwell	2-34
2-24	BWR/2 DBA Liquid Mass Inventory in the Suppression Pool	2-35
3-1	TRACB04 Nodalization of BWR/4 Reactor Assembly	3-5
3-2	BWR/4 DBA Steam Dome Pressure	3-9
3-3	BWR/4 DBA Break Flow from Suction Line connected to Vessel	3-10
3-4	BWR/4 DBA Break Flow from Drive Line in Broken Loop (Positive flow from drive line to break)	3-11
3-5	BWR/4 DBA Broken Jet Pump Discharge Flow	3-13
3-6	BWR/4 DBA Intact Jet pump Discharge Flow	3-14
3-7	BWR/4 DBA Mass Inventories in Lower Plenum and Core Normalized to Initial Mass	3-15
3-8	Regional Mass During SSTF BWR/4 Large Break LOCA Refill Test	3-17
3-9	BWR/4 DBA Mass Flow at SEO of Low Power CHAN (92 Bundles)	3-18
3-10	BWR/4 DBA Mass Flow at Top of Low Power CHAN (92 Bundles)	3-19
3-11	BWR/4 DBA Mass Flow at SEO of Average Power CHAN (584 Bundles)	3-20
3-12	BWR/4 DBA Mass Flow at Top of Average Power CHAN (584 Bundles)	3-21
3-13	BWR/4 DBA Mass Flow at SEO of High Power CHAN #1 (33 Bundles)	3-22
3-14	BWR/4 DBA Mass Flow at Top of High Power CHAN #1 (33 Bundles)	3-23
3-15	BWR/4 DBA Mass Flow at SEO of High Power CHAN #2 (55 Bundles)	3-24
3-16	BWR/4 DBA Mass Flow at Top of High Power CHAN #2 (55 Bundles)	3-25
3-17	BWR/4 DBA Void Fraction at Central Cell in the Upper Plenum	3-27
3-18	BWR/4 DBA Peak Cladding Temperature in Low Power Bundle	3-28
3-19	BWR/4 DBA Peak Cladding Temperature in Average Power Bundle	3-29
3-20	BWR/4 DBA Peak Cladding Temperature in High Power Bundle (CHAN #1)	3-30
3-21	BWR/4 DBA Peak Cladding Temperature in High Power Bundle (CHAN #2)	3-31

SUMMARY

TRAC-BWR is a best estimate code for the analysis of Boiling Water Reactor (BWR) transients. As part of the earlier BWR Refill Reflood Program, a version of TRAC-BWR (BO2) was developed for Loss-of-Coolant Accident Analysis. The model development under the FIST program was primarily aimed at extending TRAC-BWR for the analysis of other BWR transients. The main sub-tasks in this effort were to improve the numerical efficiency and computer execution time for long transients, to extend identified models to remove limitations; and to implement the models for balance of plant components developed at INEL. The end product from this effort is the TRACBO4 version of the code.

This report describes the TRACBO4 developmental assessment with BWR plant cases. A BWR/2 Design Basis Accident (DBA) and a BWR/4 DBA calculation have been performed to provide best-estimate information on the performance of these BWRs under the postulated LOCA conditions, and to assess the overall performance of TRACBO4 in realistic plant simulations.

In the BWR/2 DBA calculation, the reactor was modeled to include the containment response. The new models such as the air field and containment were tested and the results generated were found to be in agreement with engineering judgement. The containment response provides a beneficial feedback on the LOCA, as it enhances the spray heat transfer process in the latter part of the transient. The maximum Peak Cladding Temperature (PCT) was low (1053°K) and occurred early in the transient. The maximum drywell and wetwell pressures were 3.06 bars and 2.94 bars, respectively, well within the design limits.

In the BWR/4 DBA calculation, the reactor assembly was modeled with Low Pressure Coolant Injection (LPCI) water injected into the lower plenum. The core was reflooded from the refilling of the lower plenum. This scenario has the potential of producing numerical problems, known as "water packing." The code numerics and reliability were tested and the performance was found to be very satisfactory. This calculation showed that the maximum PCT was very low (630°K) and the core was completely quenched shortly after the LPCI isolation valve closed.

SECTION 1

INTRODUCTION

The Boiling Water Reactor (BWR) version of TRAC was first developed in cooperation with the Idaho National Engineering Laboratory (INEL) under the Refill/Reflood (R/R) Program. Under that program the main emphasis was on the development of models for the controlling basic phenomena in a Loss of Coolant Accident (LOCA) in the BWR and for specific BWR components (1,2). TRAC-BWR was developed to be a best estimate computer code for the thermal hydraulic conditions in a BWR LOCA. At the end of the R/R program, TRAC-BWR was extensively assessed. It was found that TRAC-BWR predicted the BWR phenomena very well, but that the computation costs were high (3).

One purpose of the FIST program has been to reduce the cost of executing TRAC and to extend its applicability to other transients. The first task was addressed by developing more implicit numerics for TRAC, whereby the Courant limitation on the time step size was removed, and by significantly improving the reliability of the code. This task is described in Volume 1 of this document and has led to a significant reduction in the cost of executing TRAC both in terms of computer time as well as engineering time.

The second task of extending the applicability of TRAC involved implementation of a noncondensable gas (air) field, a boron transport model accounting for stratification and mixing, a model for the two phase level, generalized heat transfer between the components and component models for the containment, turbine and heat exchanger. These models are described in Volume 2 of this document. Figure 1-1 shows the evolution of various versions of TRAC, the GE and INEL developments, and the interactions between various versions of TRAC.

During the development of the improved numerical methods and new models for TRAC, the models were individually tested. This developmental assessment is reported together with the respective models in Volumes 1 and 2 of this document. The purpose of this document is to describe the assessment of TRAC for BWR plant cases. This not only tests the phenomena and component interactions in TRAC but also provides valuable information on the performance of the BWR. For this purpose calculations have been performed for a BWR/2 and a BWR/4 plant.

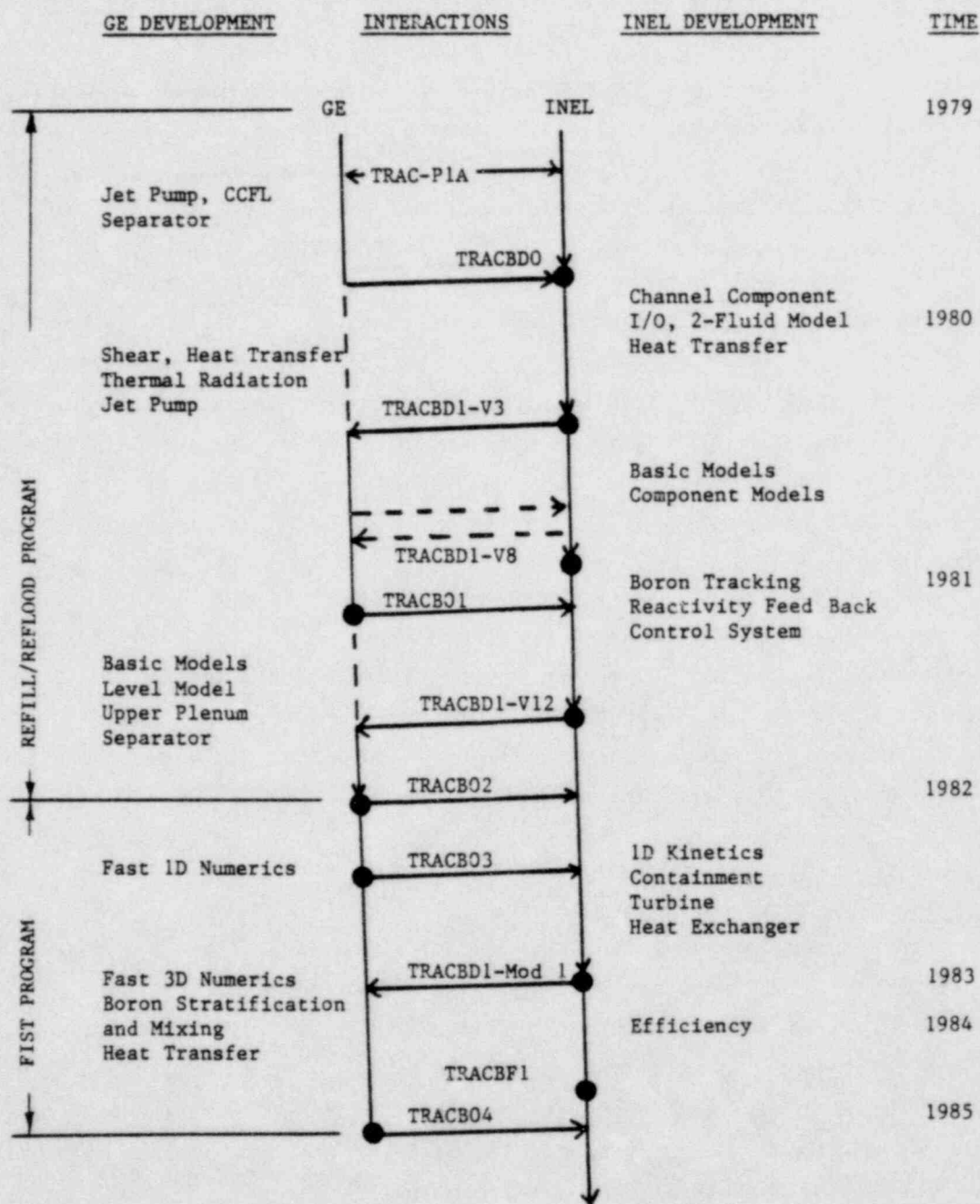


Figure 1-1. Major Milestone in TRAC-BWR Development

The assessment calculation for the BWR/2 plant is a large break (DBA) LOCA with containment response. In this case, both the reactor assembly and the containment are modeled. The main objectives of this calculation are to test new models such as the air field and containment, to assess the effects of containment feedback, and to provide best estimate BWR/2 DBA calculational results. The descriptions, nodalization and results of the BWR/2 DBA case are presented in Section 2.

The assessment calculation for the BWR/4 plant is also a large break (DBA) LOCA. In this case, the Low Pressure Coolant Injection (LPCI) water is injected into the lower plenum through the recirculation drive line and the core is reflooded from the refilling of the lower plenum. The objectives of this calculation are to test the code numerics and reliability, and to provide best estimate BWR/4 DBA calculational results. The descriptions, nodalization and results of the BWR/4 DBA case are presented in Section 3.

SECTION 2

BWR/2 RECIRCULATION LINE BREAK

One of the major differences that distinguish the BWR/2 plant from later BWR plants is in the design of recirculation loops. In the BWR/2 plants, there are no jet pumps in the vessel downcomer and the recirculation line connects the downcomer to the lower plenum. Further, the pipe diameter in the recirculation line is larger than for jet pump plants. As a result of this design, a large break can be postulated in the recirculation line leading to the depletion of inventory from the lower plenum and core. A larger break causes the BWR/2 vessel to depressurize faster and reach containment pressure level sooner (i.e., before the time of peak cladding temperature is reached) than jet pump plants under Design Basis Accident (DBA) conditions. At low vessel pressures, the break flows as well as core thermal hydraulics would be affected by the containment response.

This section describes the TRACB04 developmental assessment case for a BWR/2 recirculation line break (DBA). A typical BWR/2 plant was modeled including the reactor vessel and containment. The vessel is a BWR/2 213-inch vessel with 560 fuel bundles. The containment is a Mark-1 design corresponding to a BWR/2-213 vessel. The containment model includes drywell, wetwell and suppression pool.

2.1 OBJECTIVES OF BWR/2 DBA CALCULATION

The objectives of this calculation are to:

- (a) Assess the overall performance of TRACB04 in a system calculation with containment interaction;
- (b) Test out the containment model and air field option implemented in TRACB04 in a realistic plant simulation;
- (c) Assess the response of core thermal hydraulics to the containment pressurization due to LOCA and;
- (d) Provide best estimate BWR/2 DBA calculational results.

2.2 CASE DESCRIPTIONS

The general assumptions, initial conditions and TRAC nodalization used in the BWR/2 DBA calculation are described below.

2.2.1 Assumptions

The general assumptions used in the calculation are summarized in Table 2-1. The break size, available Emergency Cooling systems and trip timing in Table 2-1 are typical conditions for a BWR/2 DBA.

2.2.2 Initial Conditions

The initial conditions used in the calculation are summarized in Table 2-2. The bundle powers in the hot bundle, average bundle and peripheral bundle are 5.1 MW, 3.6 MW and 1.76 MW, respectively. This power distribution corresponds to radial power peakings of 1.45, 1.026 and 0.50, respectively. The axial peaking is 1.50 for all bundles, and the Maximum Planar Linear Heat Generation Rate (MAPLHGR) in the hot bundle is 9.87 kW/ft.

2.2.3 TRAC Nodalization

Figure 2-1 shows the TRAC nodalization of the reactor assembly for a typical BWR/2-213 plant. The reactor vessel is simulated using a VESSEL component with 13 axial levels, 4 radial rings and 1 azimuthal sector, for a total of 52 VESSEL 3-dimensional cells. This nodalization is guided by considerations of reactor geometry and governing phenomena. The axial levels are located to provide geometric definition of principal regions (e.g., lower plenum) and to provide connecting points for components (e.g., guide tubes). The outer radial ring models the downcomer region and the three inner radial rings describe the radial subdivision of the core and bypass region inside the shroud, fuel channels, and the associated guide tubes and steam separators.

The reactor core occupies two axial levels (Levels 6 and 7) in the inner three radial rings. Inner ring #1 corresponds geometrically to 60 bundles located around the core center. These 60 bundles are assumed to be the hot bundles with bundle power of 5.1 MW. They are modeled by two High Power CHANs with 24 bundles in one CHAN component and 36 bundles in the other CHAN component. This utilizes the new capability in TRACB04 to have multiple channels in the same vessel cell. This grouping allows the two subgroups of hot bundles to have different flow configurations, if calculated. The outer ring #3 contains all 76 peripheral bundles which have smaller inlet orifices. These 76 bundles with an assumed bundle power of 1.76 MW are modeled by one Low Power CHAN component. The central ring #2 represents the remaining 424 bundles. These bundles with an assumed bundle power of 3.6 MW are modeled by one Average Power CHAN component.

Table 2-1

BWR/2 DBA CALCULATION - ASSUMPTIONS

Break size (sq ft)	4.66 (guillotine break)
Break location	Discharge line
Problem time zero	Normal water level
Power scram	Time 0.0 second
Feedwater pump trip	Time 0.0 second; Linearly closed in 1.0 second
Recirculation pump trip	Time 0.0 second
MSIV trip	Time 0.0 second; 0.5 seconds delay; 5.0 seconds closure time
ECCS	2 LPCS available
LPCS trip	Level 1 + 32 seconds
LPCS permissive pressure	286 psig
LPCS water	From suppression pool
Containment spray	Not available for First few minutes of LOCA
Decay heat	ANSO .79 + 0%

Table 2-2

BWR/2 DBA CALCULATION - INITIAL CONDITIONSPOWER

Total reactor power (MW)	1969.
Hot bundle power (MW)	5.098
Average Bundle power (MW)	3.607
Peripheral bundle power (MW)	1.759
Max. linear power rate (kW/ft)	11.0
Gap conductance ($\text{W/m}^2\text{K}$)	5600.0

FLOW

Total steam flow (kg/s)	993.6
Total recirculation flow (kg/s)	7700.0
Initial suppression pool temperature	305.2°K (90.0°F)
Initial drywell temperature	33.0°K (140.0°F)

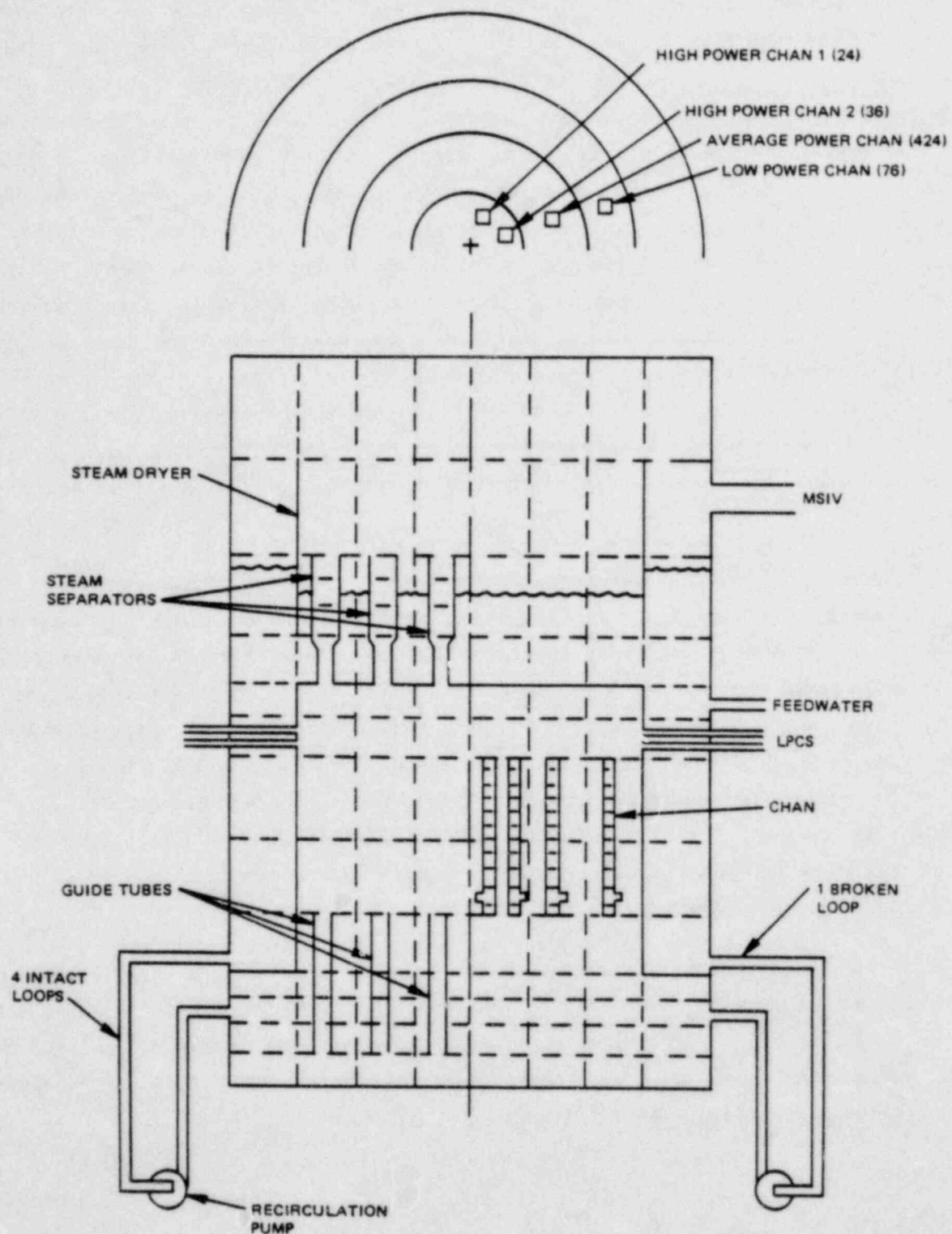


Figure 2-1. TRAC Nodalization of BWR/2 Reactor Assembly

Three PIPE components, one in each of the three inner rings, are used to model the 137 guide tubes in a BWR/2-213 plant. These PIPE components represent the 15, 106 and 16 guide tubes in Rings 1, 2 and 3, respectively. Similarly three SEPARATOR components, one in each of the three inner rings, are used to model the 151 steam separators. The numbers of steam separators are 14, 99 and 38 in Rings #1, 2 and 3, respectively. The 5 recirculation loops are modeled by one broken loop and one intact loop in the TRAC calculation. Each loop consists of one suction PIPE component, one recirculation PUMP component and one discharge Pipe component. The intact loop in the TRAC model represents 4 real intact loops with appropriate flow area and volume. The ECCS lines are modeled by 4 PIPE components, each one is connected to a FILL component with appropriate pressure versus velocity table to simulate the LPCS flow rate. The other ends of these PIPE components are connected to the peripheral cell in the upper plenum, representing spray nozzles with different angle and elevation. The ECC spray sources and distributions are calculated by the upper plenum model (2).

Figure 2-2 shows the schematic of TRACB04 nodalization of the BWR/2 vessel and containment. The drywell is modeled by a COMPARTMENT component of the containment model. The drywell compartment interacts with the vessel through heat transfer from the vessel wall and through pipe BREAK components located in the drywell. The solid heat masses such as drywell skirt, concrete shield wall, and vent pipes are modeled by three HEAT STRUCTURES of the containment model. The wetwell including the suppression pool is modeled by a COMPARTMENT component. The wetwell compartment interacts with the vessel through ECC FILL components which pump ECC water from the suppression pool. Heat masses such as vent headers, downcomers, and wetwell wall are modeled by two HEAT STRUCTURES.

A PASSIVE JUNCTION of the containment model is used to model the vent pipes connecting the drywell and wetwell. The downcomer exits are simulated at an elevation of 3 feet below the initial suppression pool surface. A second PASSIVE JUNCTION is used to model the vacuum breakers between the drywell and wetwell with vacuum breaker opening pressure of 0.5 psig.

2.3 RESULTS

The break in the recirculation line for the BWR/2 leads to a rapid depressurization of the reactor vessel, primarily due to the large flow area of the external recirculation line. Most of the break flow is from the lower plenum through the discharge end of the recirculation line and the remaining part of the break flow is from the downcomer through the pump to the break location.

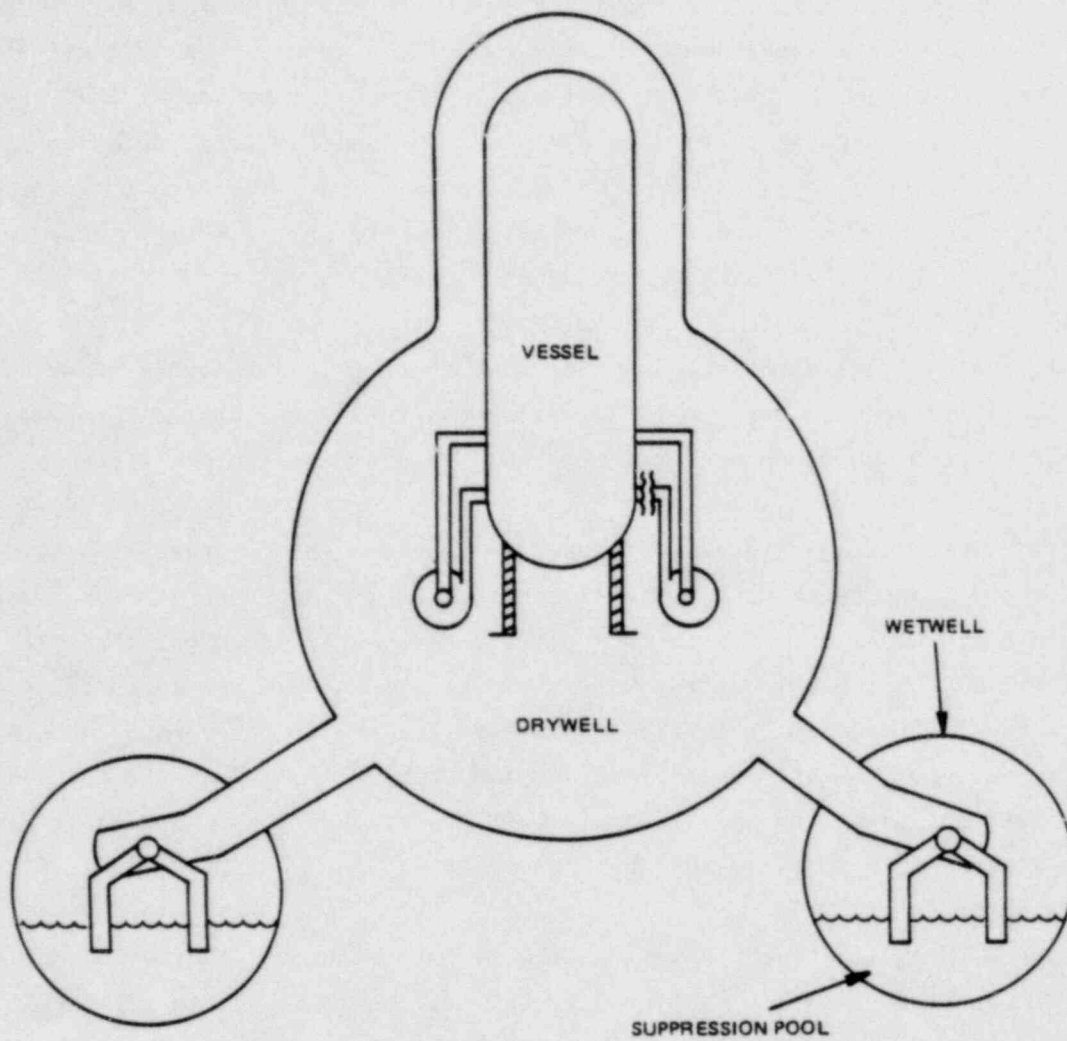


Figure 2-2. Schematic of TRACB04 Nodalization of BWR/2 Vessel and Component

The large break flow from the lower plenum causes an immediate flow reversal at the core inlet and a subsequent boiling transition and heat up of the fuel. However, shortly after the break the reversal of the core flow causes the liquid in the upper plenum and separators to drain through the fuel bundles. This liquid downflow causes the low and average power bundles to quench and turns over the temperature in the high power bundles. Indeed, the maximum temperature of 1053°K observed during this first peak is the final peak cladding temperature.

After the draining of the upper plenum, the high power bundles heat up again until the core spray comes on. Thereafter the fuel temperatures level off with a balance between the decay heat and the heat transfer rate in the spray cooling mode.

The large initial break flow causes the containment to pressurize to 2-1/2 times atmospheric pressure, which is the final pressure for both the reactor vessel and the containment. Later in the transient, as the core spray comes on, more steam is condensed on the subcooled spray water than is produced in the core region. This causes the lower plenum break flow to reverse and an air-steam mixture enters the reactor vessel. The air concentrates in the upper plenum, where it reduces the condensation rate on the spray water. This causes the spray water to retain its subcooling as it enters the fuel bundles.

The high equilibrium pressure in the system together with the low temperature of the ECC water as it enters the fuel are the main reasons for the relatively low peak cladding temperature. The liquid flow to the bundles in the absence of CCFL at the upper tie plate is given by the spray distribution. In the present analysis, this was calculated by the upper plenum model in TRAC, yielding an average of 0.50 kg/s-bundle available to the high power bundles. The reactor minimum bundle flow would be expected to be lower than this value.

The sequence of important events of this calculation is summarized in Table 2-3. Reactor scram, recirculation pump trip, and feedwater pump trip occurred immediately following the pipe break. The main steam isolation valve (MSIV) trip also occurred at time zero. The MSIV has a delay time of 0.5 seconds and closure time of 5.0 seconds. It fully closed at 5.5 seconds into the transient.

Table 2-3

SEQUENCE OF EVENTS FOR BWR/2 DBA

<u>Event</u>	<u>Time (sec)</u>
Recirculation line break	0.0
Power scram	0.0
Feedwater pump trip	0.0
Recirculation pump trip	0.0
MSIV closure started	0.5
Feedwater off	1.0
L1 trip	2.1
Onset of lower plenum flashing	3.1
Onset of Bypass Flashing	4.0
MSIV fully closed	5.5
Suction pipe uncover	8.0
Discharge pipe uncover	11.0
ECC spray on	34.1
Onset of back flow in break	66.0
Water level in lower plenum reflooded to discharge pipe	122.0
Core hot spot starts cooling	130.0

Figure 2-3 shows the steam dome pressure for the BWR/2 DBA transient. The steam dome depressurized rapidly at a rate of 4 bars per second for the first 3 seconds. The rate of depressurization slowed down between 3 to 8 seconds due to the MSIV closure and the onset of lower plenum flashing (3.1 seconds). After the suction pipe uncover (8 seconds) and discharge pipe uncover (11 seconds), the depressurization rate again increased to about 2 bars per second. At the end of this calculation (201 seconds) the system pressure had dropped to an equilibrium value of 2.3 bars (33.4 psia).

The break flows from the break pipe connecting to the recirculation pump and from the break pipe connecting to the vessel are shown in Figures 2-4 and 2-5, respectively. The times of uncover for the suction pipe and discharge pipe are indicated distinctly by the sudden reduction in break flows. The break flow from the recirculation pump side (Figure 2-4) remained positive throughout the transient, with a magnitude of about 20 kg/s from 60 seconds to 132 seconds. The break flow from the vessel side became negative (i.e., flow from drywell to vessel) starting at 66 seconds. The break flow was about -30 kg/s from 66 seconds to 100 seconds, and then gradually reduced to zero at 122 seconds. This period of negative flow introduced air and steam mixture from the drywell into the vessel.

After the water level in the lower plenum reflooded to the discharge pipe exit elevation at 122 seconds, the break flow from the vessel side became periodically positive with flow magnitude ranging from 200 kg/s to 800 kg/s.

Figures 2-6 through 2-13 show the mass flows at the inlet (side entry orifice) and top of the Low Power CHAN, Average Power CHAN, High Power CHAN #1 and High Power CHAN #2. These CHAN components simulate 76 peripheral bundles, 424 average power bundles, 24 and 36 high power bundles correspondingly. For all types of bundles, the flows at SEO changed from positive (up flow) to negative (down flow) immediately following the pipe break, with magnitudes of 50% of the initial value for the Low Power CHAN (Figure 2-6), and 80% of the initial value for other CHANS (Figures 2-8, 2-10 and 2-12).

The flows at the top of bundles decreased rapidly from their initial positive values to negative flows at about 6 seconds after the pipe break (Figures 2-7, 2-9, 2-11 and 2-13). These figures also show large down flow at top of bundles for the time period from 11 to 20 seconds. This was due to the fact that after the discharge pipe uncover, the lower plenum pressure dropped rapidly and the upper plenum subsequently depleted through the lower plenum.

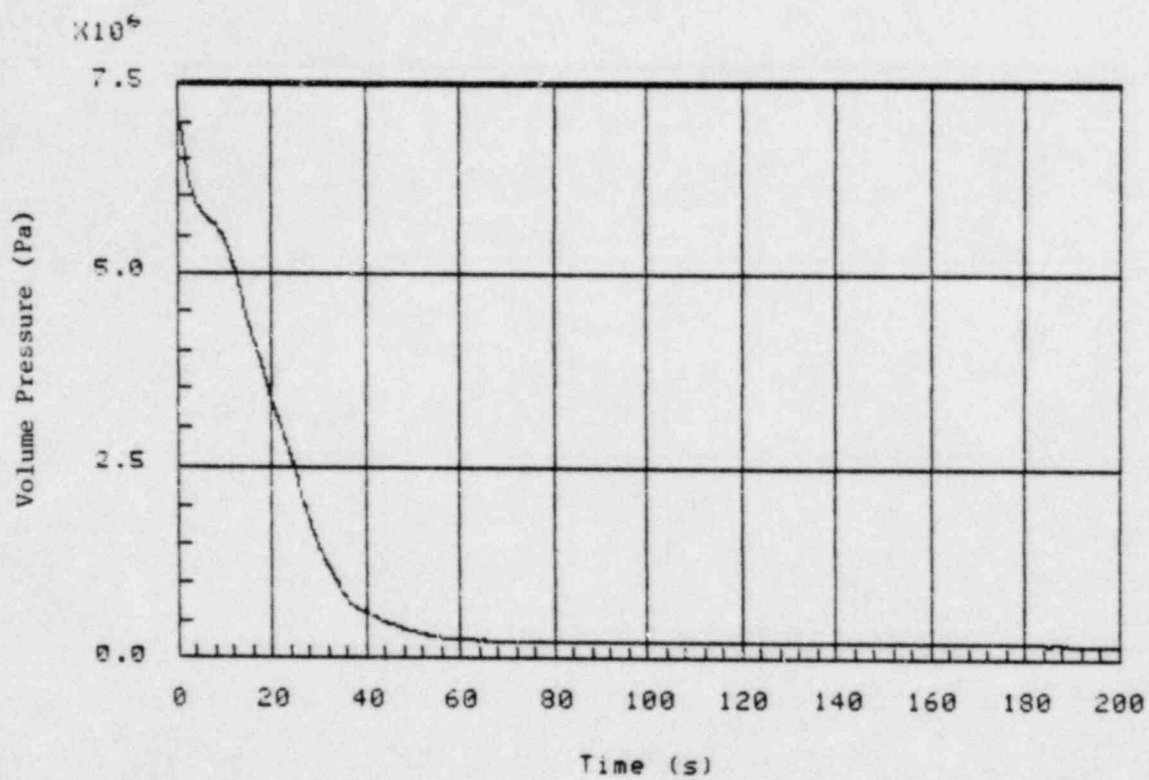


Figure 2-3. BWR/2 DBA Steam Dome Pressure

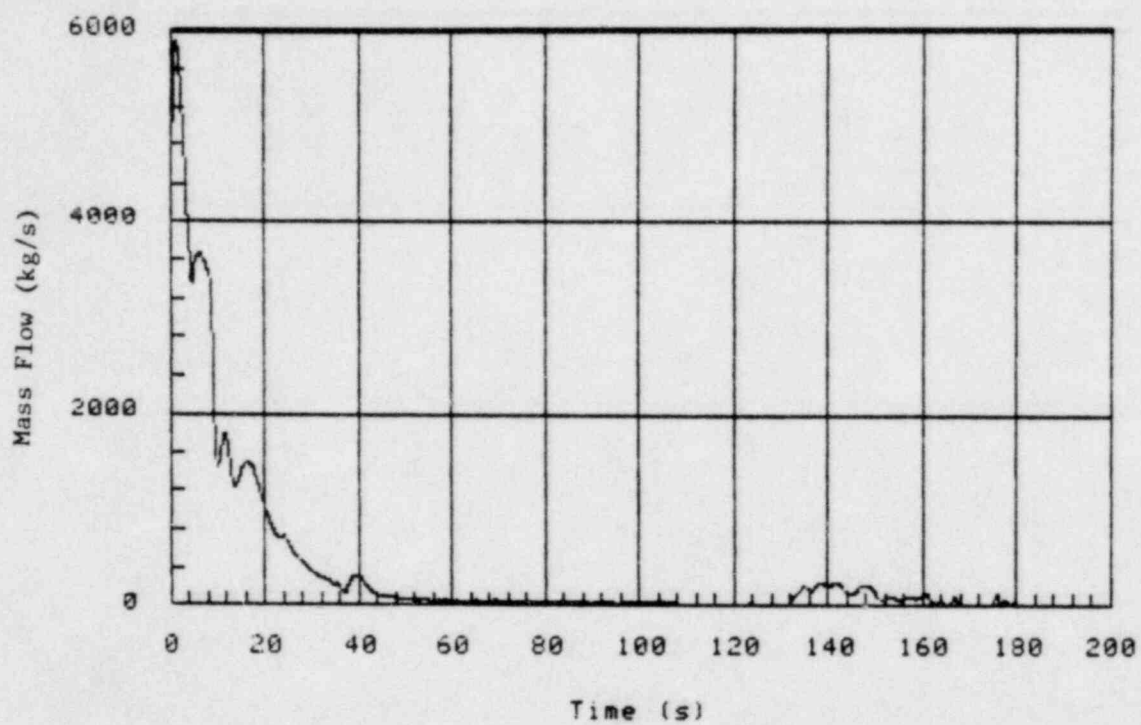


Figure 2-4. BWR/2 DBA Break Flow from the Recirculation Pump Side

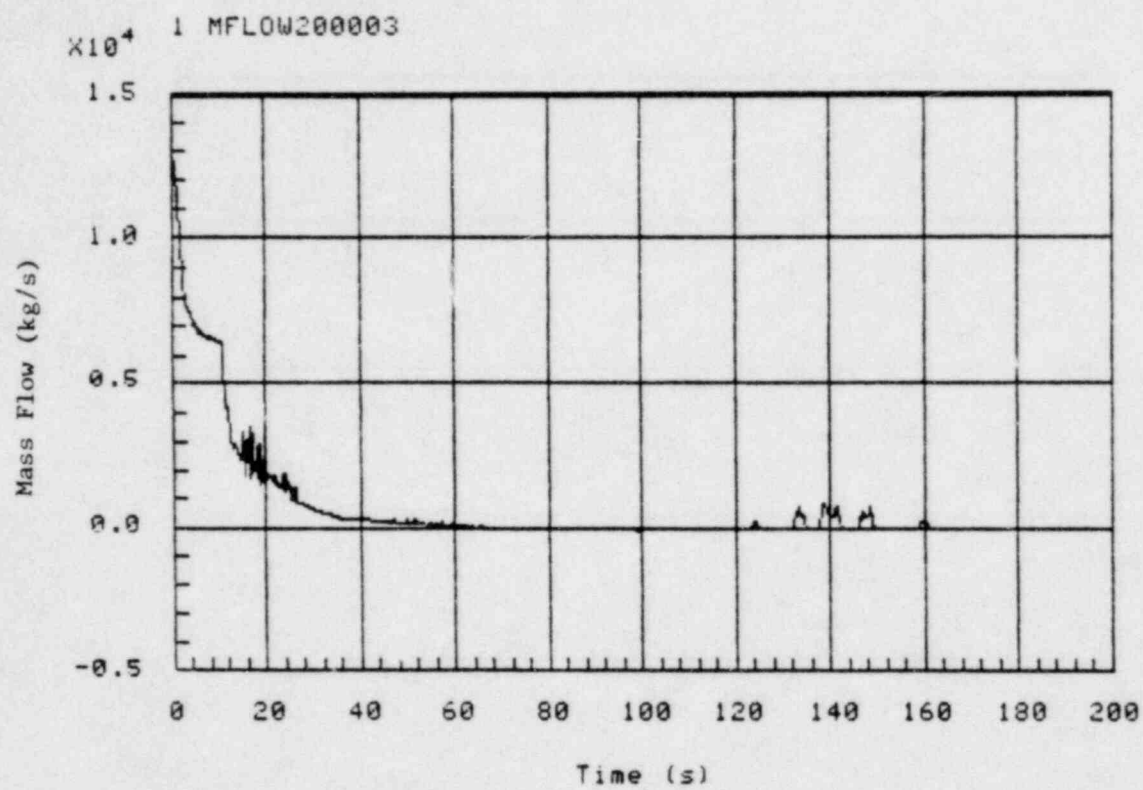


Figure 2-5a. BWR/2 DBA Break Flow from the Vessel Side

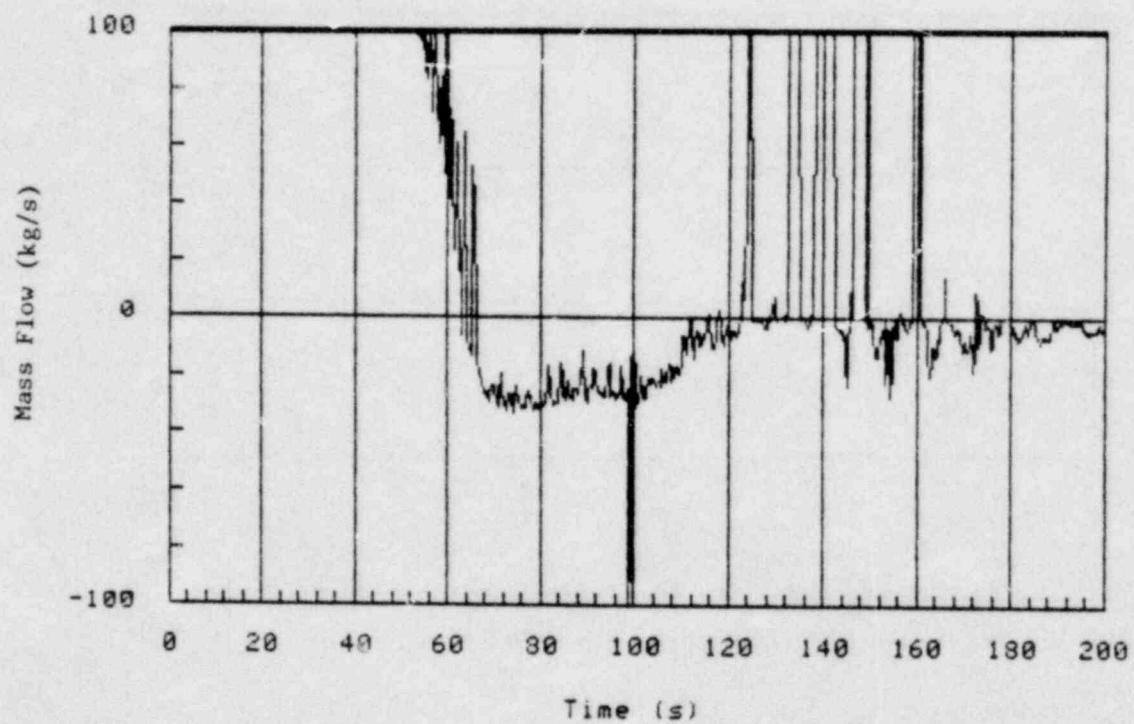


Figure 2-5b. BWR/2 DBA Break Flow from the Vessel Side (Blow-up Scale)

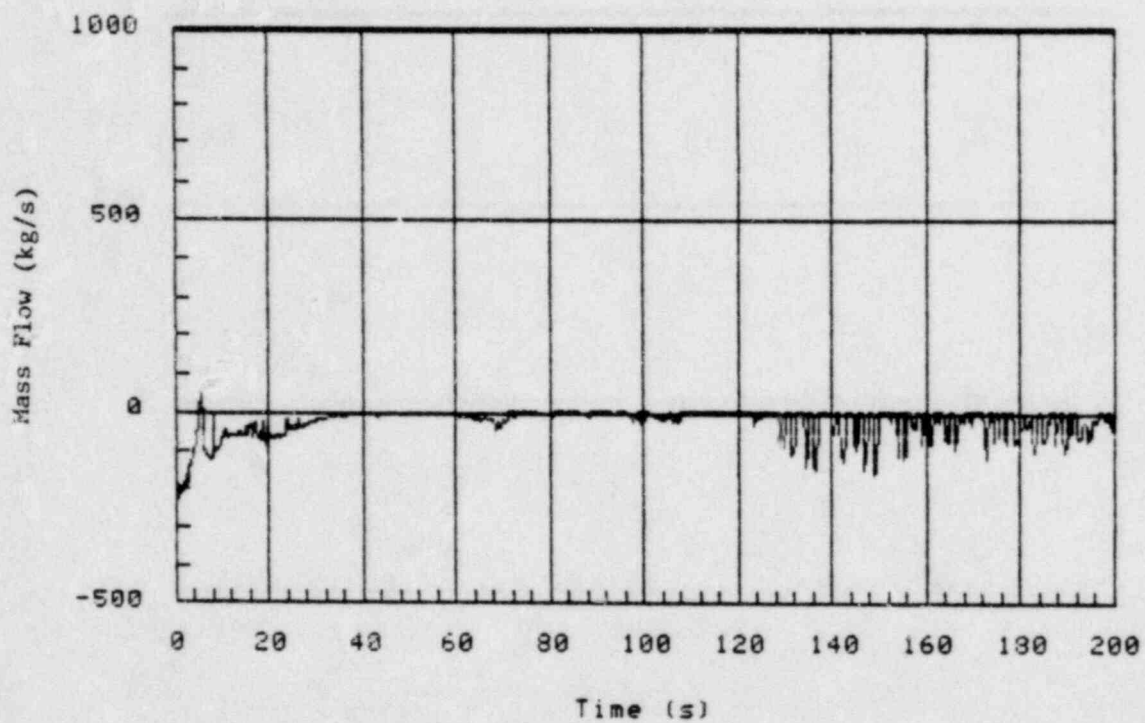


Figure 2-6. BWR/2 DBA Mass Flow at SEO of Low Power
CHAN (76 Bundles)

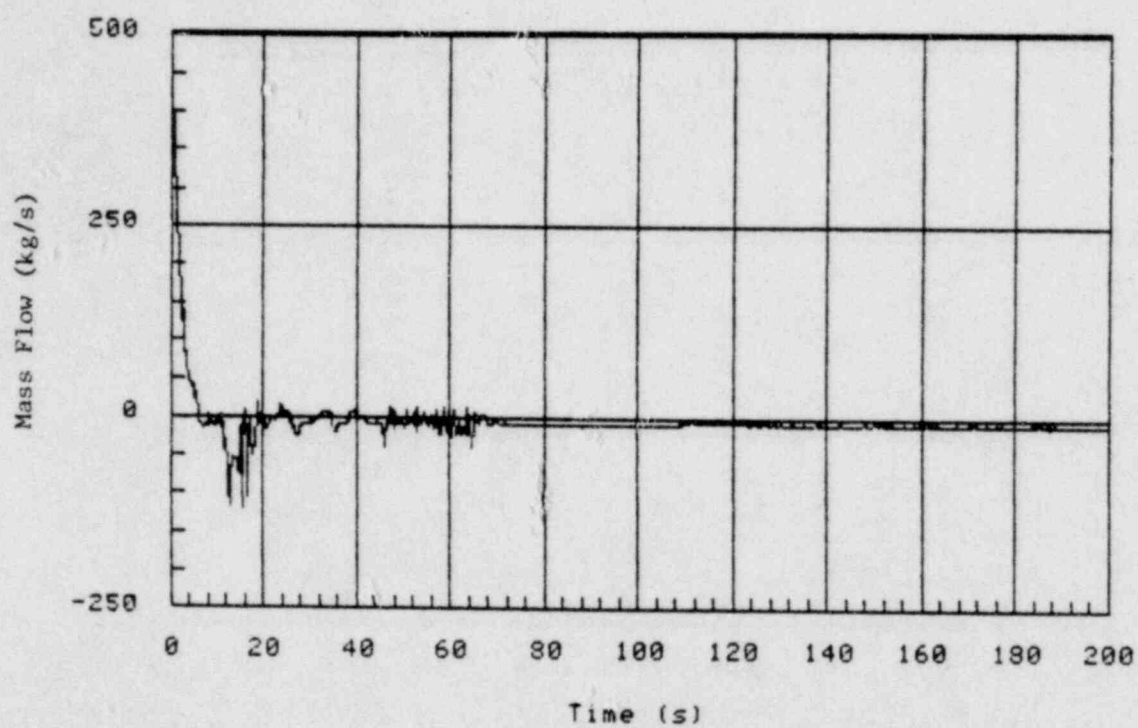


Figure 2-7. BWR/2 DBA Mass Flow at Top of Low Power
CHAN (76 Bundles)

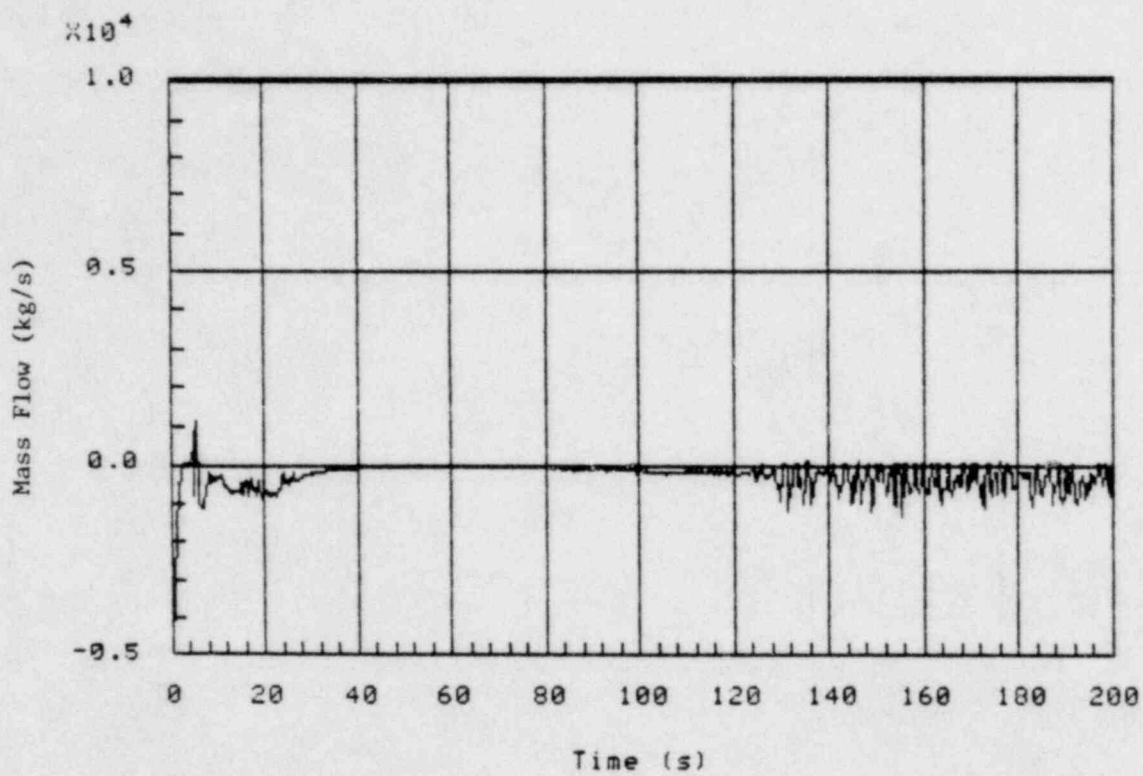


Figure 2-8. BWR/2 DBA Mass Flow at SEO of Average Power
CHAN (424 Bundles)

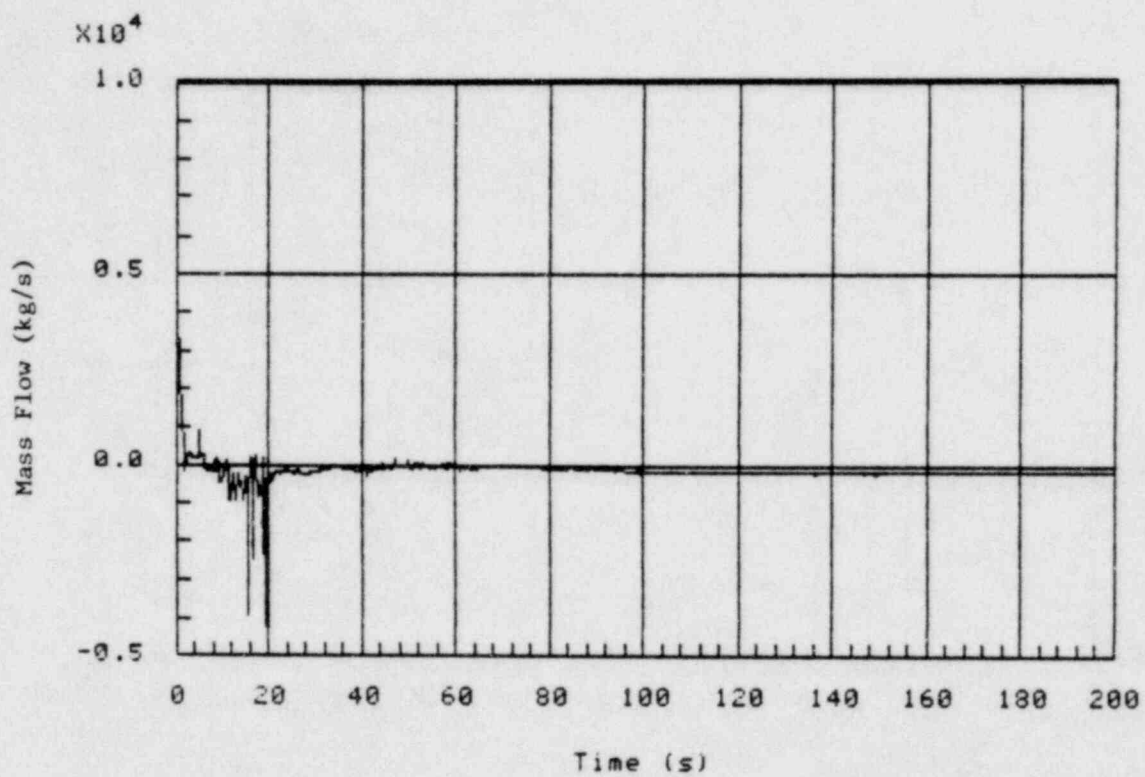


Figure 2-9. BWR/2 DBA Mass Flow at Top of Average Power
CHAN (424 Bundles)

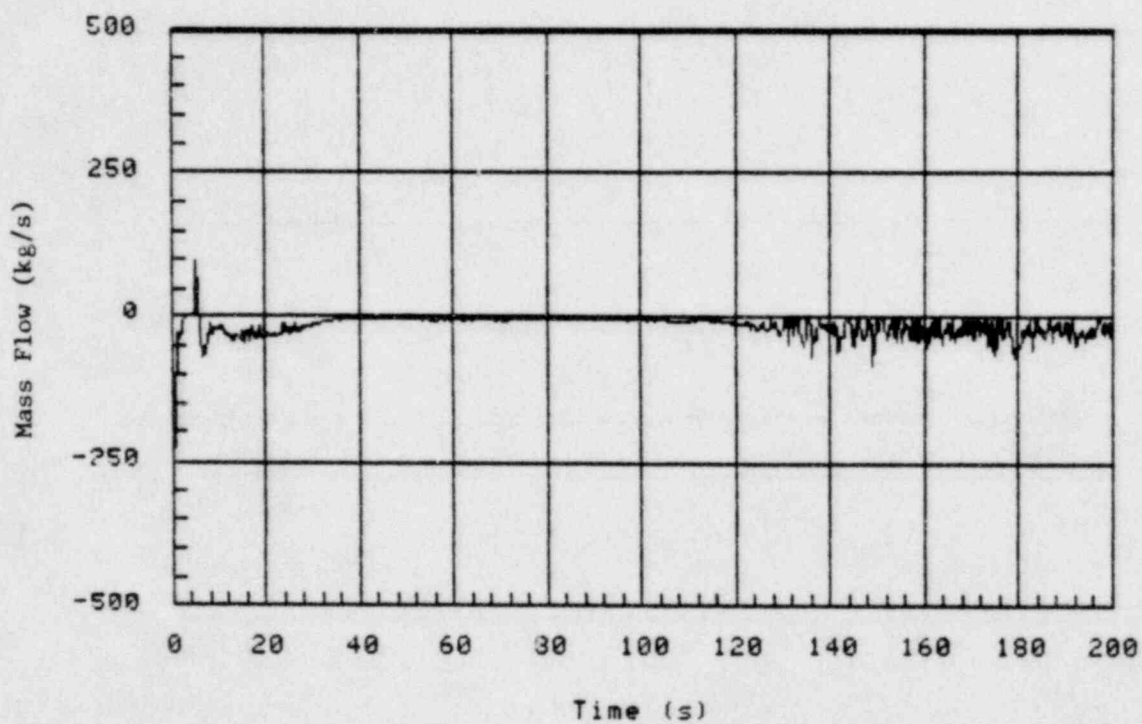


Figure 2-10. BWR/DBA Mass Flow at SEO of High Power
CHAN #1 (24 Bundles)

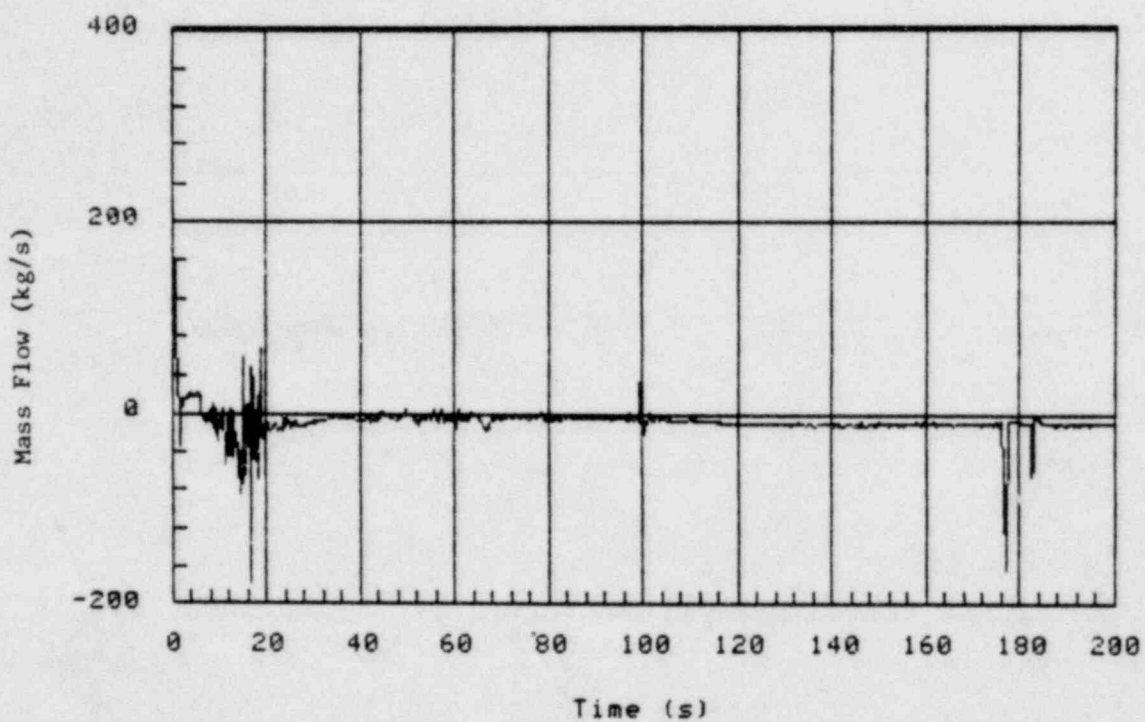


Figure 2-11. BWR/2 DBA Mass Flow at Top of High Power
CHAN #1 (24 Bundles)

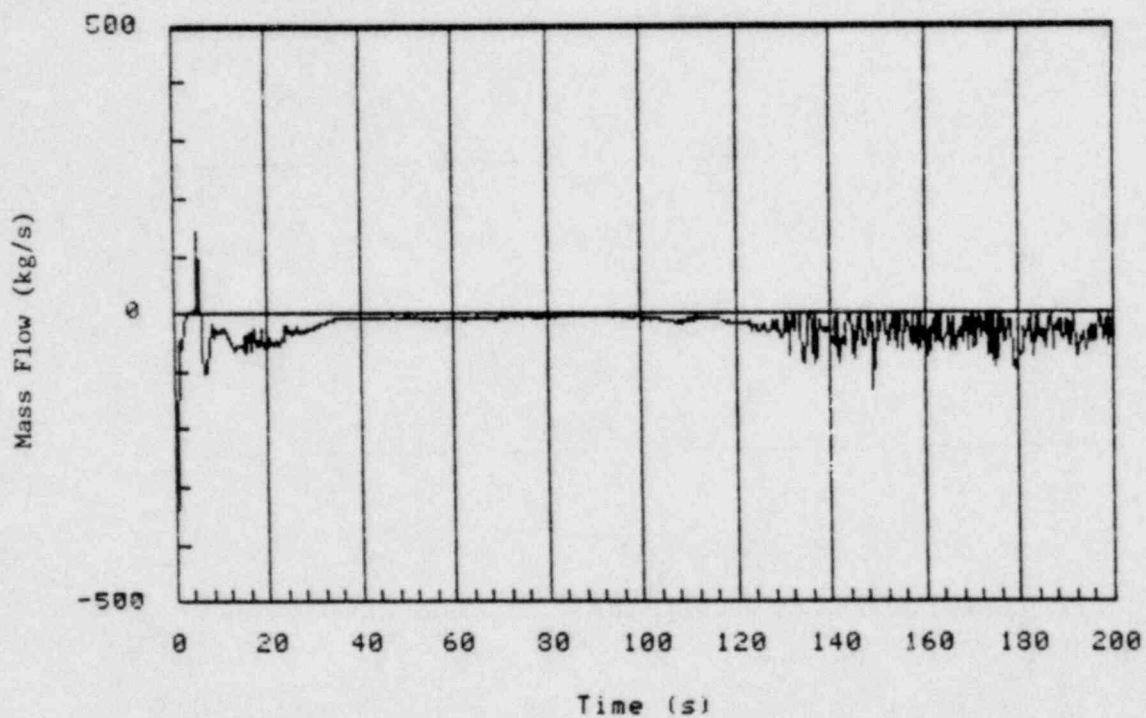


Figure 2-12. BWR/2 DBA Mass Flow at SEO Of High Power
CHAN #2 (36 Bundles)

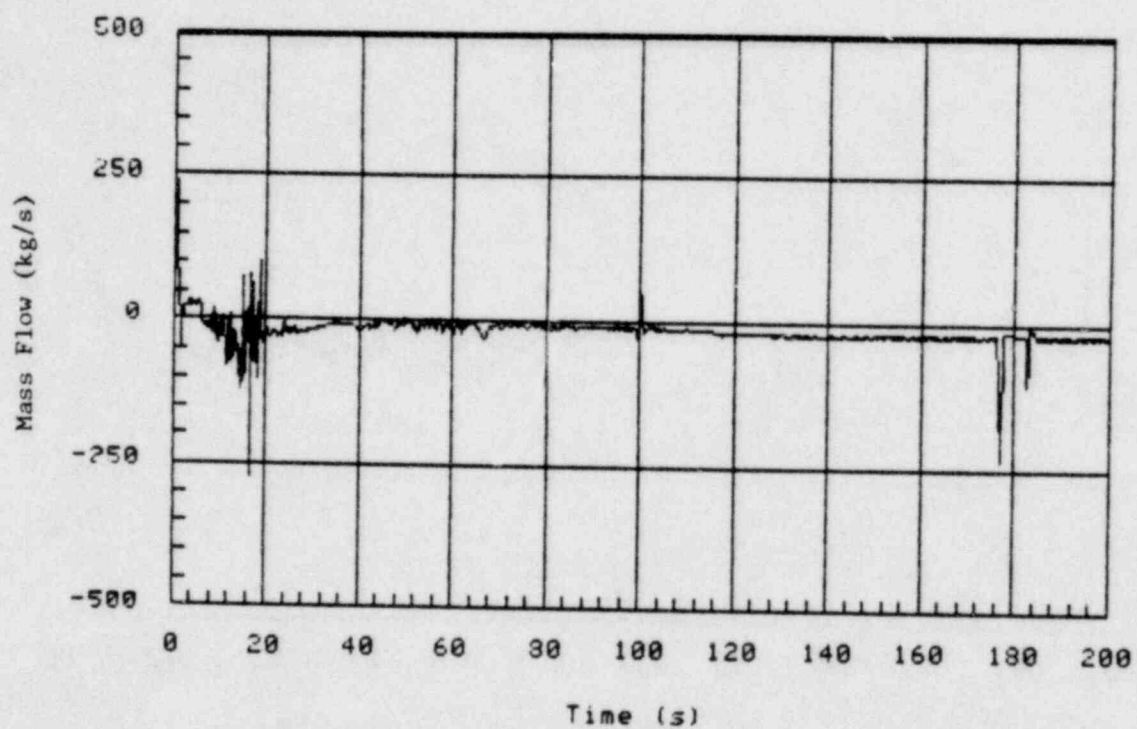


Figure 2-13. BWR/2 DBA Mass Flow at Top of High Power
CHAN #2 (36 Bundles)

For the peripheral bundles, the SEO flow (Figure 2-6) was co-current downward after the discharge pipe uncover (11 seconds). At 72 seconds (6 seconds after the start of back flow of steam and air from drywell to lower plenum through break pipe), the SEO flow switched to counter-current with steam and air flowing upward. The SEO flow remained generally counter-current from 72 seconds to the end of the run. The flow at the top of bundle (Figure 2-7) was counter-current from 20 seconds to the end of the run.

For the average power bundles, the SEO flow (Figure 2-8) was co-current downward from 6 to 110 seconds. After 110 seconds, the SEO flow showed oscillations with periods of counter-current flow with steam and air flowing upward. The flow at the top of bundles (Figure 2-9) was co-current downward from 11 to 39 seconds, then switched to counter-current flow from 39 to 100 seconds. After 100 seconds, the flow became generally co-current downward with occasional periods of counter-current flow.

For the high power bundles, the flow conditions (per bundle wise) calculated by the High Power CHAN #1 and #2 are almost identical (Figures 2-10 to 2-13). The SEO flow was co-current downward from 6 seconds to the end of run, except for intermittent, counter-current flow occurring after 130 seconds. The flow at the top of bundles was generally co-current downward from 11 to 60 seconds, then switched to counter-current flow from 60 to 116 seconds. After 116 seconds, the flow oscillated back and forth between co-current down and counter-current flows.

Figure 2-14 shows the partial air pressures at Level 8 of the vessel (bottom level of upper plenum, cell 1 connected to the exit of High Power CHANs, cell 2 to Average Power CHAN, and cell 3 to Low Power CHAN). The air flowed from drywell into lower plenum through the pipe break and then flowed upward through the Low Power CHAN (peripheral bundles) into cell 3 of the upper plenum. The air then flowed radially inward into cells 2 and 1. The presence of air in the upper plenum reduced the condensation by the ECC spray water and increased the subcooling in the water flowing into the bundles. Figure 2-15 shows the total and partial air pressures in Cell 1 (central cell) at the bottom level of the upper plenum. Figure 2-16 shows the water subcooling (liquid temperature - saturation temperature based on total pressure) of the corresponding cell. It clearly indicates that the upper plenum water subcooling increases as the air content increases. The water at top of Average Power and High Power CHANs became subcooled at 100 and 116 seconds, respectively. At this time, the flow at top of these bundles changed from counter-current flow to co-current down flow. After 120 seconds, the air/steam mixture at the lower level of upper plenum contained about 80 to 90% air.

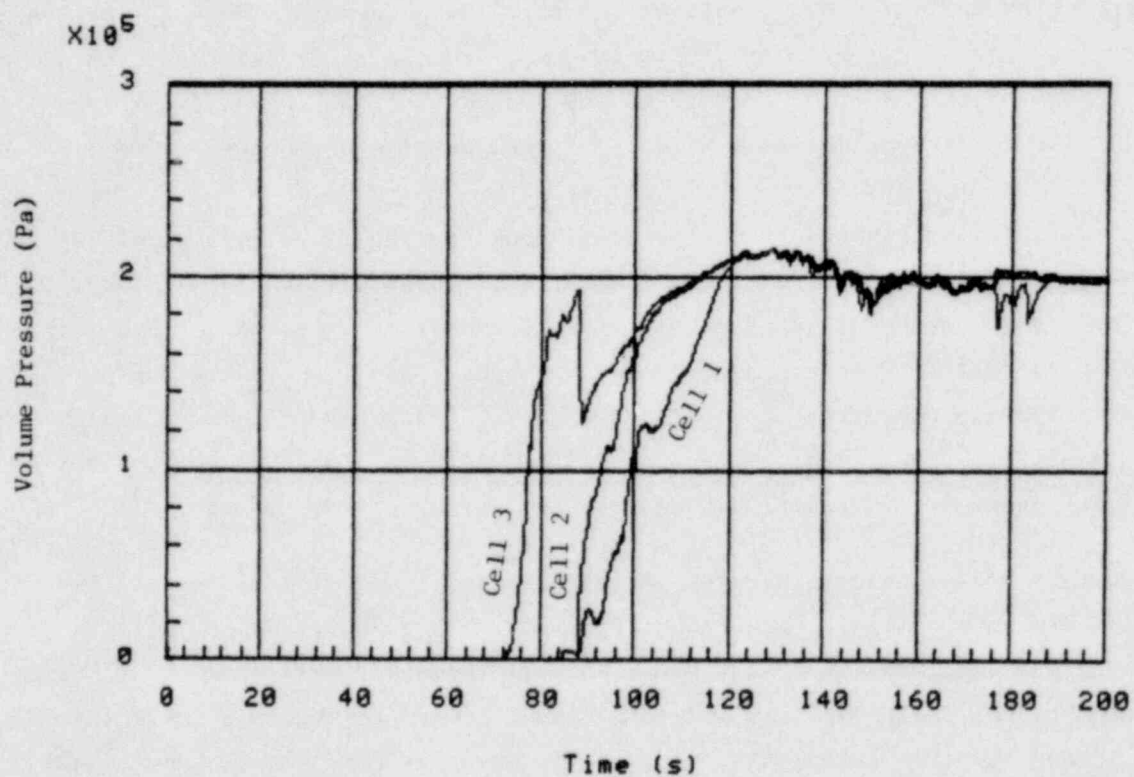


Figure 2-14. BWR/2 DBA Partial Air Pressures at Bottom Level of Upper Plenum

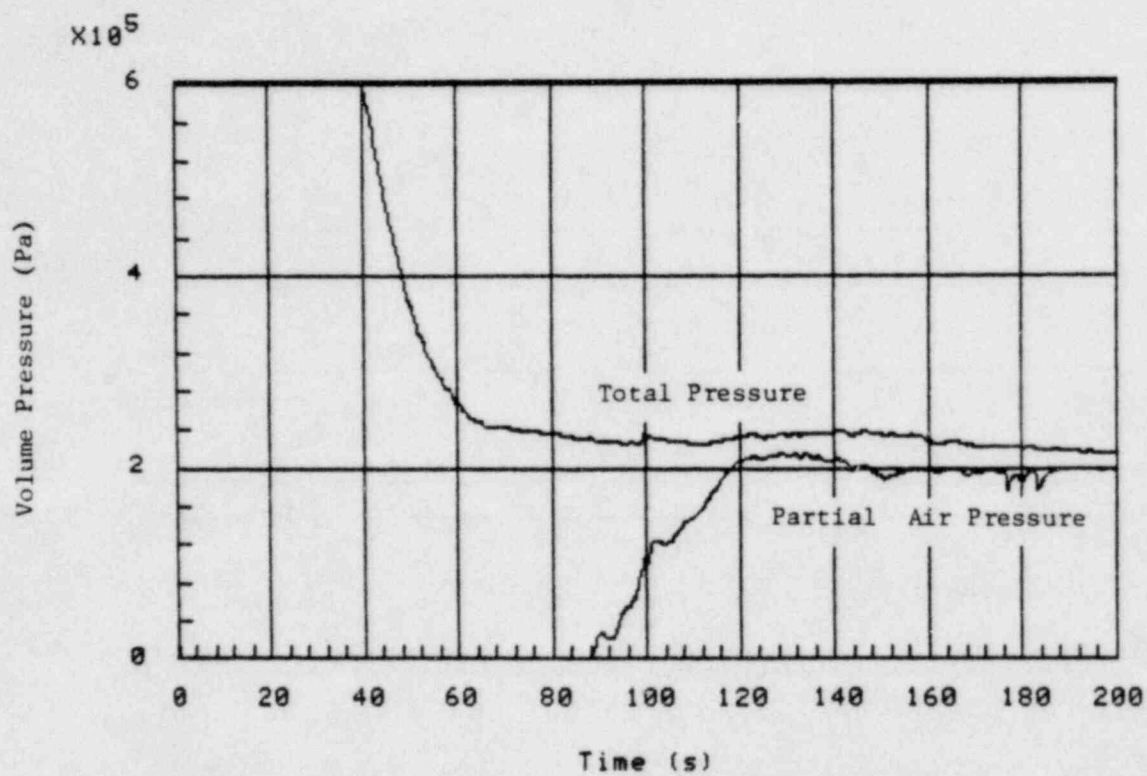


Figure 2-15. BWR/2 DBA Total and Partial Air Pressures in Cell 1 at Bottom Level of Upper Plenum

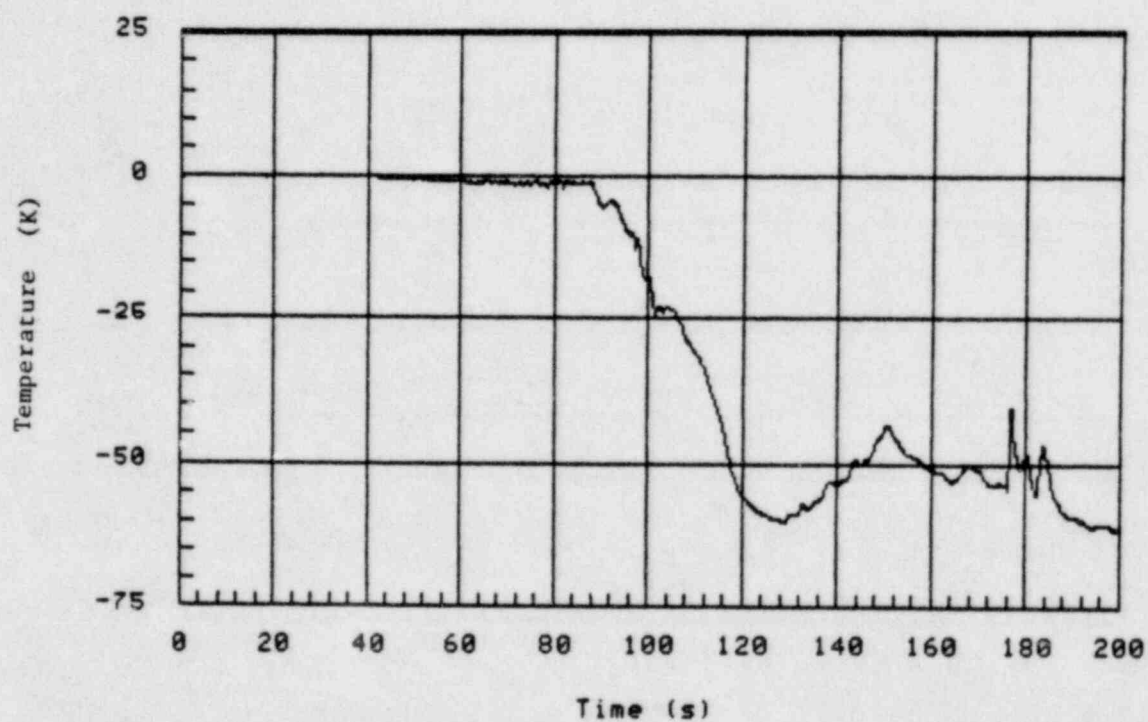


Figure 2-16. BWR/2 DBA Water Subcooling in Cell 1 at Bottom Level of Upper Plenum

Figures 2-17 to 2-20 show the Peak Cladding Temperatures (PCT) in the low power, average power and high power bundles. The PCT calculated for the High Power CHAN #1 and #2 are almost identical in this case. Shortly after the pipe break, all bundles heated up rapidly as the core dried out. At 11 seconds into the transient, the PCTs for all bundles turned around as large amounts of liquid flowed from the upper plenum into the bundles (Figures 2-7, 2-9, 2-11 and 2-13). This down flow was the result of the discharge pipe uncovering which allowed a large amount of steam to escape from the break. At this time the PCTs reached the maximum values of 609°K, 850°K and 1053°K for the low, average and high power bundles.

The low power and average power bundles quenched completely at 72 and 80 seconds, respectively. The hot spot in the high power bundle started cooling at 130 seconds, and maintained an average temperature close to 1000°K for the rest of the calculation.

Figure 2-21 shows the total and partial air pressure in the drywell. Immediately after the pipe break, the drywell pressure rose rapidly and reached a peak value of 3.06 bars (44.44 psia) at 25 seconds. The air in the drywell was completely pushed into the wetwell at about 18 seconds. At 31 seconds, the vacuum breakers between the the wetwell and drywell opened and air started to flow back into the drywell from the wetwell (Figure 2-21). The liquid mass inventory in the drywell is shown in Figure 2-22.

Figure 2-23 shows the total and partial air pressure in the wetwell. Immediately after the pipe break, the wetwell was pressurized rapidly by the displaced drywell air and a small amount of drywell steam that escaped from the condensation process in the suppression pool. The wetwell reached a maximum pressure of 2.94 bars (42.60 psia) at 30 seconds. The mass inventory in the suppression pool is shown in Figure 2-24. The mass inventory increased for the time period from 0 to 40 seconds due to the condensation of drywell steam. After the ECCS came on at 34.1 seconds, the mass inventory decreased at a constant rate of 500 kg/s, which was about the rate of ECC flow into the upper plenum.

2.4 MAIN OBSERVATIONS

From the BWR/2 DBA calculation a number of observations concerning the performance of the TRACE04 code and BWR/2 during a LOCA can be made:

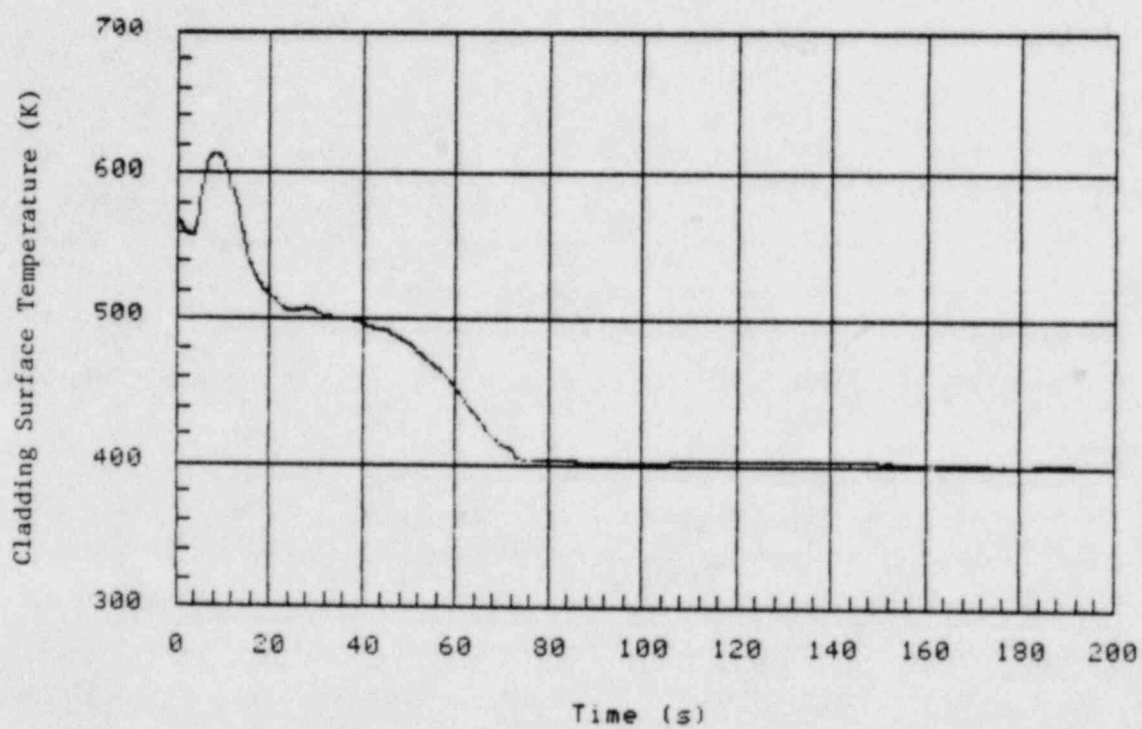


Figure 2-17. BWR/2 DBA Peak Cladding Temperature in Low Power Bundle

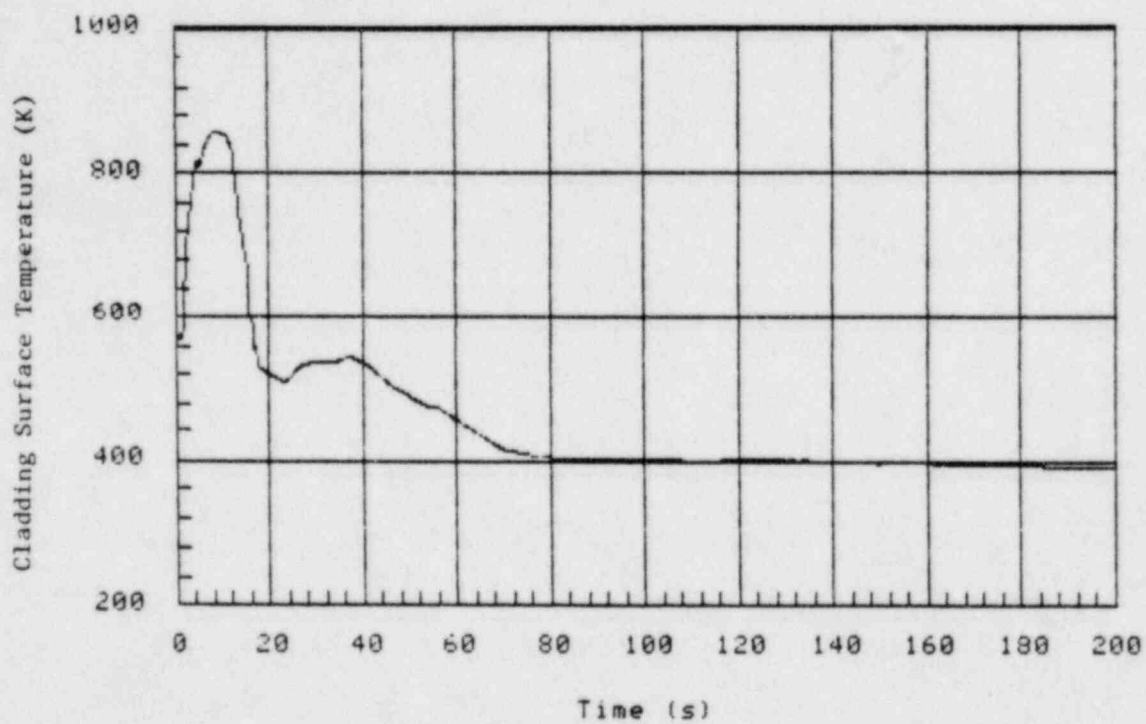


Figure 2-18. BWR/2 DBA Peak Cladding Temperature in Average Power Bundle

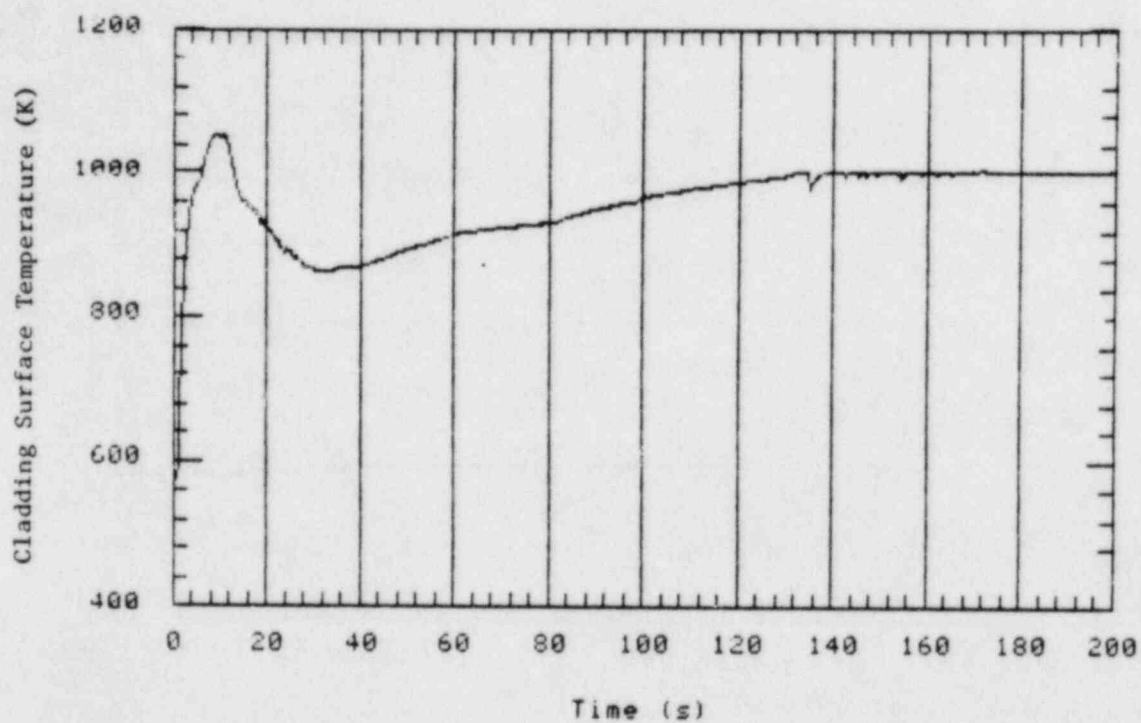


Figure 2-19. BWR/2 DBA Peak Cladding Temperature in High Power Bundle (CHAN #1)

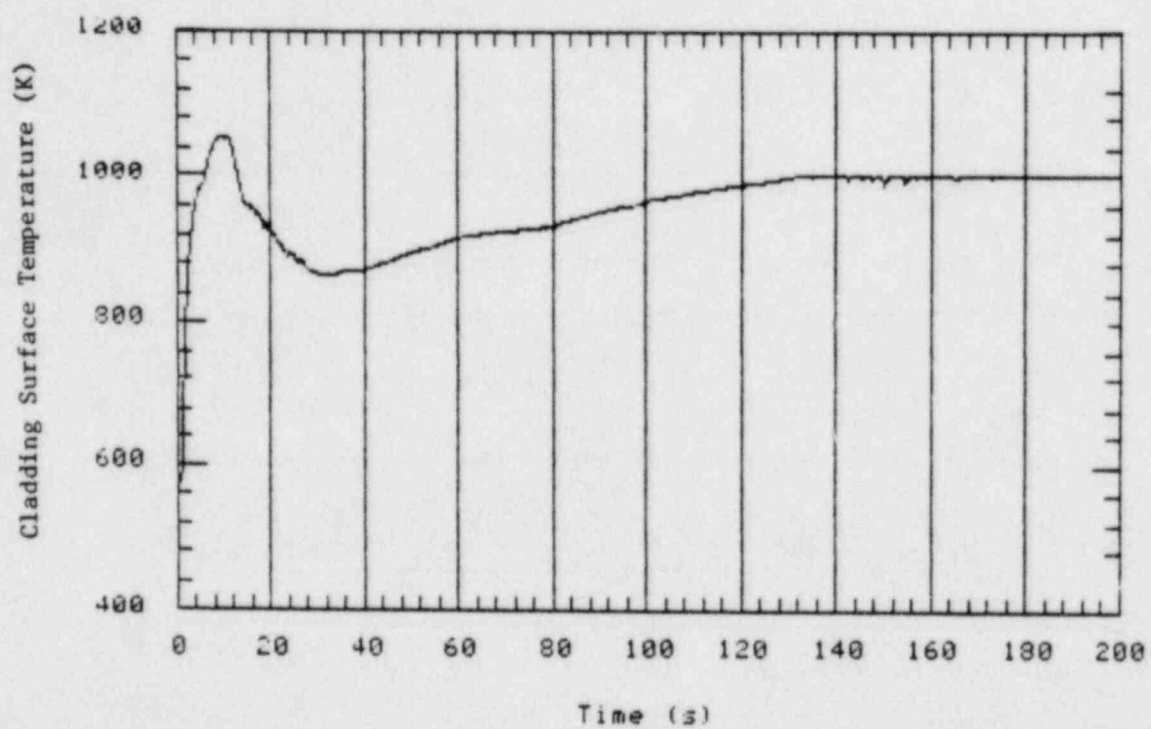


Figure 2-20. BWR/2 DBA Peak Cladding Temperature in High Power Bundle (CHAN #2)

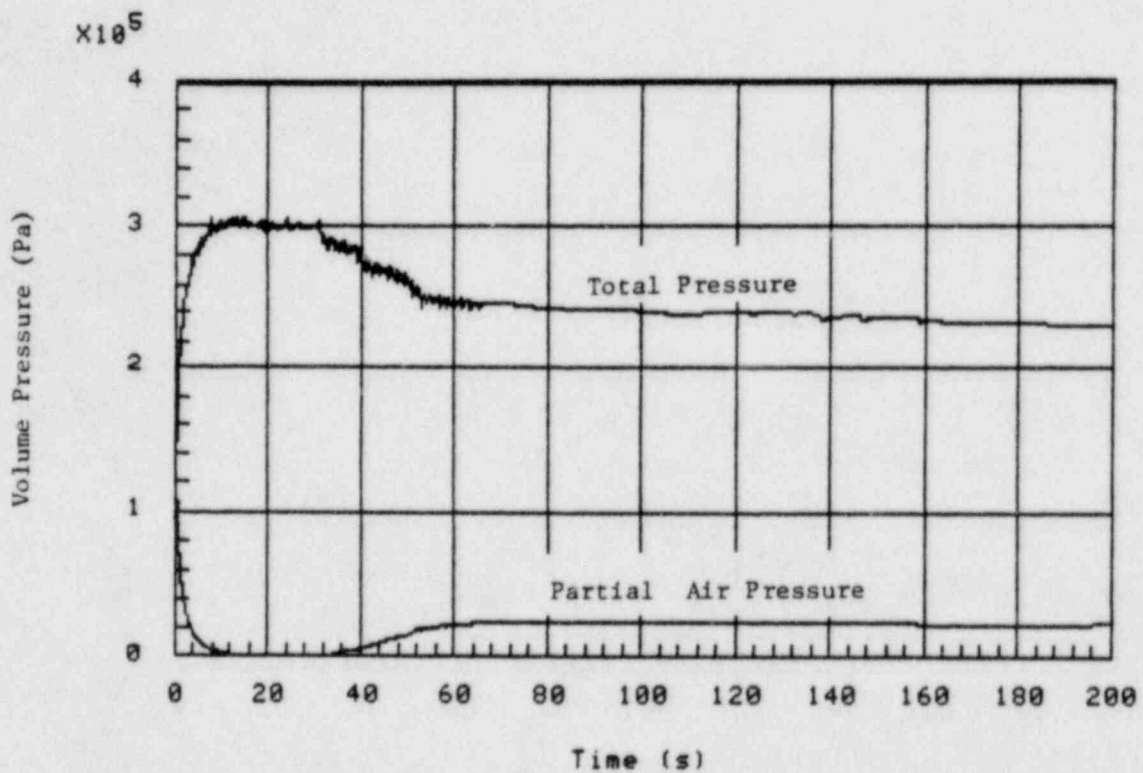


Figure 2-21. BWR/2 DBA Total and Partial Air Pressure in the Drywell

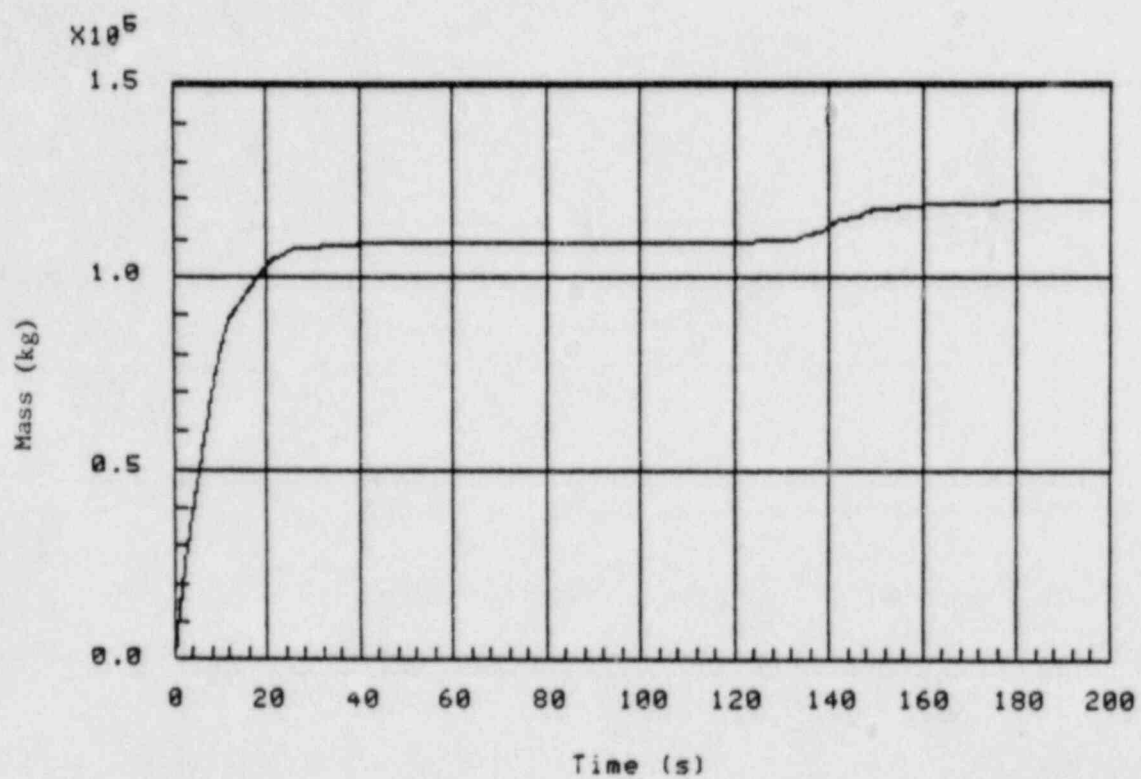


Figure 2-22. BWR/2 DBA Liquid Mass Inventory in the Drywell

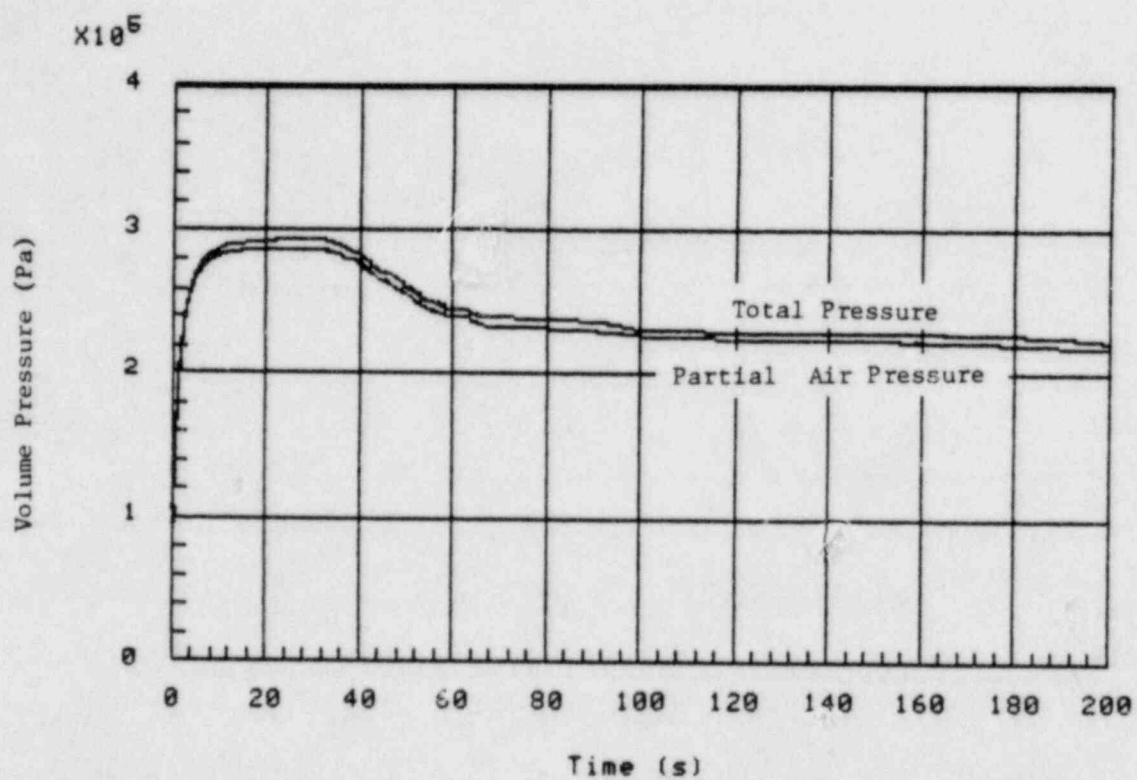


Figure 2-23. BWR/2 DBA Total and Partial Air Pressure in the Wetwell

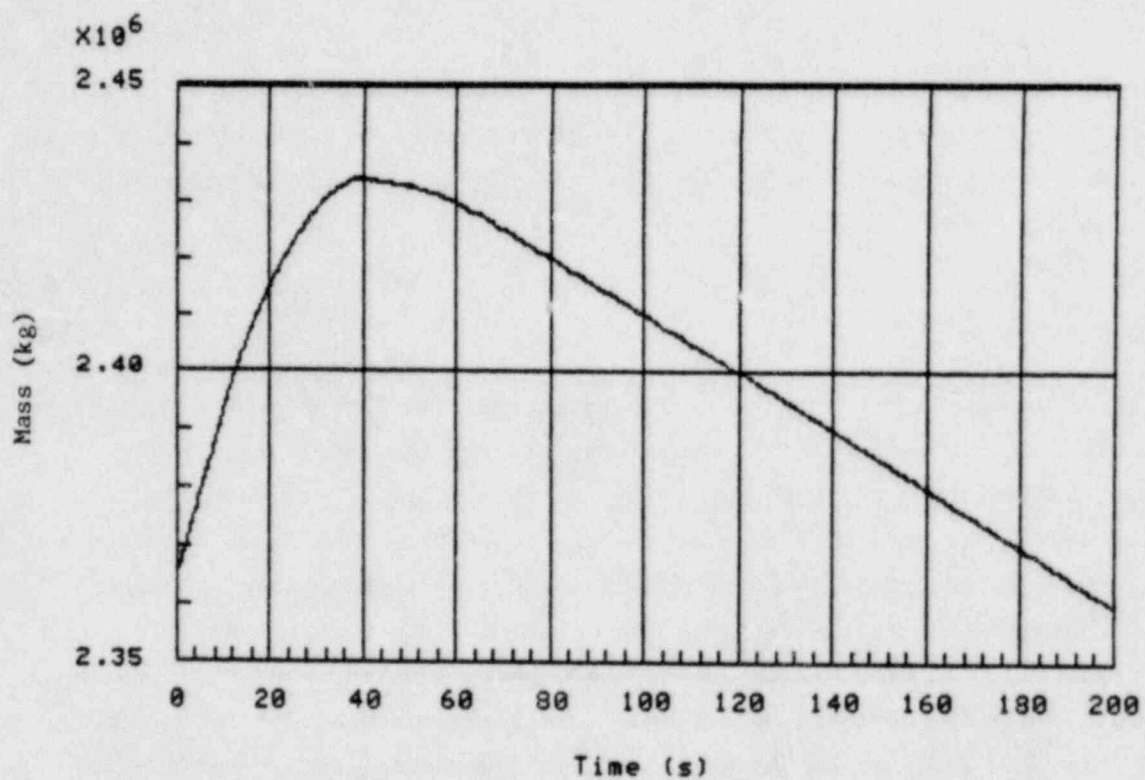


Figure 2-24. BWR/2 DBA Liquid Mass Inventory in the Suppression Pool

TRACB04 performance

- o The overall performance of TRACB04 has been improved making it significantly easier to use than previous versions of the TRAC-BWR code. This is primarily due to the fast numerics and the reliability improvements developed under the FIST program.
- o The new models implemented under the FIST Program, such as the noncondensable gas (air) model and the containment model are correctly implemented and properly predict the performance of the containment and the effect of air.
- o The generalized heat transfer allowing several channels in one vessel cell is implemented correctly. In this case however, very little difference was observed between the two hot channels in the central vessel ring.

BWR/2 LOCA characteristics

- o The containment feedback has a significant effect on the LOCA transient. The pressurization of the containment causes the final reactor vessel pressure after the blowdown to be approximately 2.4 bar rather than 1 bar commonly assumed when no containment feedback is considered. At 2.4 bar, the CCFL restrictions for the same steam flow at the upper tie plate is considerably less, and no CCFL occurs at the upper tie plate. Consequently, no level builds up in the upper plenum and the liquid downflow into the fuel bundles is determined by the spray distribution in the upper plenum. Later in the transient, the condensation capacity of the ECC water exceeds the steam generation in the core and an air/steam mixture flows from the containment back into the vessel. There the air collects where the condensation takes place, i.e. in the upper plenum. As a result, the condensation in the upper plenum is gradually reduced and the spray water retains part of the subcooling as it enters the fuel channels.

- o The high vessel pressure and relatively large flow of subcooled ECC water into the high power fuel bundles produces good spray cooling heat transfer (an Appendix K type spray cooling heat transfer coefficient based on the saturation temperature of $5.0 \text{ Btu/hr-F-ft}^2$ is observed). With this heat transfer, the maximum temperature during the spray cooling mode is approximately 1000°K . The flow to a given bundle could be less resulting in a somewhat higher local PCT. The early peak due to the boiling transition immediately following the break is 1053°K , making this the PCT.
- o The maximum containment pressures were 3.06 bar in the drywell and 2.94 bar in the wetwell.

SECTION 3

BWR/4 RECIRCULATION LINE BREAK

The BWR/4 100% recirculation line break was analyzed to assess the TRACB04 overall performance in a system calculation when the core is reflooded from the direct refilling of the lower plenum. This section describes the objectives and results of the BWR/4 DBA assessment calculation. In this calculation, the reactor assembly of a typical BWR/4 plant is modeled. The vessel is a BWR/4 251-inch vessel with 764 fuel bundles.

3.1 OBJECTIVES OF BWR/4 DBA CALCULATION

The objectives of this calculation are to:

- (a) Assess the overall performance of TRACB04 in a system calculation with core reflooding;
- (b) Test numerics and code reliability during refilling and reflooding processes;
- (c) Provide best-estimate BWR/4 DBA calculational results.

3.2 CASE DESCRIPTIONS

The general assumptions, initial conditions and TRAC nodalizations used in the BWR/4 DBA calculation are described below.

3.2.1 Assumptions

The general assumptions used in the calculation are summarized in Table 3-1. The worst single failure is a failure of the battery that powers the HPCI, 2 LPCIs and 1 LPCS. As a result, only 1 LPCS and 2 LPCIs are assumed to be available, one LPCI in each loop. LPCI water is injected into the lower plenum through the recirculation drive line. The LPCI isolation valves, which are placed in the recirculation drive line to prevent loss of LPCI coolant through the break, close when the vessel pressure is below 275 psia, with a delay time of 30 seconds. The break size, available Emergency Cooling systems and trip timing listed in Table 3-1 are typical conditions for a BWR/4 DBA.

Table 3-1

BWR/4 DBA CALCULATION - ASSUMPTIONS

Break size (sq ft)	4.067 (100%)
Break location	Suction line
Problem time zero	Normal water level
Power Scram	Time 0.0 second
Feedwater pump trip	Time 0.0 second; linearly closed in 1.0 second
Recirculation pump trip	Time 0.0 second
MSIV trip	Time 0.0 second; 0.5 seconds delay; 5 seconds closure time
ECCS	1 LPCS 2 LPCIs (one in each loop)
LPCS trip	Vessel pressure drops below 445 psia
LPCS permissive pressure (psi)	290.
LPCI trip	Vessel pressure drops below 445 psia +10 seconds delay time
LPCI Permissive pressure (psi)	295.
LPCI isolation valve closed	Vessel pressure drops below 275 psia + 30 seconds delay time
Decay heat	ANSO .79 + 0%
ECCS water temperature	322. K (120 F)

3.2.2 Initial Conditions

The initial conditions used in the calculation are summarized in Table 3-2. The bundle powers in the hot bundle, average bundle and peripheral bundle are 6.03 MW, 4.39 MW and 2.16 MW, respectively. This power distribution corresponds to radial power peakings of 1.40, 1.02 and 0.50. The axial peaking is 1.54 for all bundles, and the Maximum Planar Linear Heat Generation Rate (MAPLHGR) in the hot bundle is 12.0 kW/ft.

3.2.3 TRAC Nodalization

Figure 3-1 shows the TRAC nodalization of the reactor assembly for a typical BWR/4-251 plant. The reactor vessel is simulated using a VESSEL component with 11 axial levels, 4 radial rings and 1 azimuthal sector for a total of 44 VESSEL 3-dimensional cells. This nodalization is guided by considerations of reactor geometry and governing phenomena. The axial levels are located to provide geometric definition of principal regions (e.g., lower plenum) and to provide connecting points for components (e.g., jet pumps). The outer radial ring models the downcomer region and the three inner radial rings describe the radial subdivision of the core and bypass region, inside the shroud and the associated guide tubes, fuel channels and steam separators.

The reactor core occupies two axial levels (levels 4 and 5) in the inner three radial rings. Inner ring #1 corresponds geometrically to 88 bundles located around the core center. These 88 bundles are assumed to be the hot bundles with bundle power of 6.03 MW. They are modeled by two High Power CHANs with 33 bundles in High Power CHAN #1 and 55 bundles in High Power CHAN #2. This utilizes the new capability in TRACB04 to have multiple channels in the same vessel cell. This grouping allows the two subgroups of hot bundles to have different flow configurations, if calculated. The outer ring #3 contains all 92 peripheral bundles which have smaller inlet orifices. These 92 bundles with assumed bundle power of 2.16 MW are modeled by one Low Power CHAN component. The central ring #2 represents the remaining 584 bundles. These bundles with assumed bundle power of 4.39 MW are modeled by one Average Power CHAN component.

Table 3-2

BWR/4 CALCULATION - Initial Conditions

POWER

Total reactor power (MW)	3293.
Hot bundle power (MW)	6.03
Average bundle power (MW)	4.39
Peripheral bundle power (MW)	2.16
Max. linear power rate (kW/ft)	13.4
Gap conductance ($\text{W/m}^2 \text{ K}$)	5600.0

FLOW

Total steam flow (kg/s)	1637.
Total core flow (kg/s)	13088.

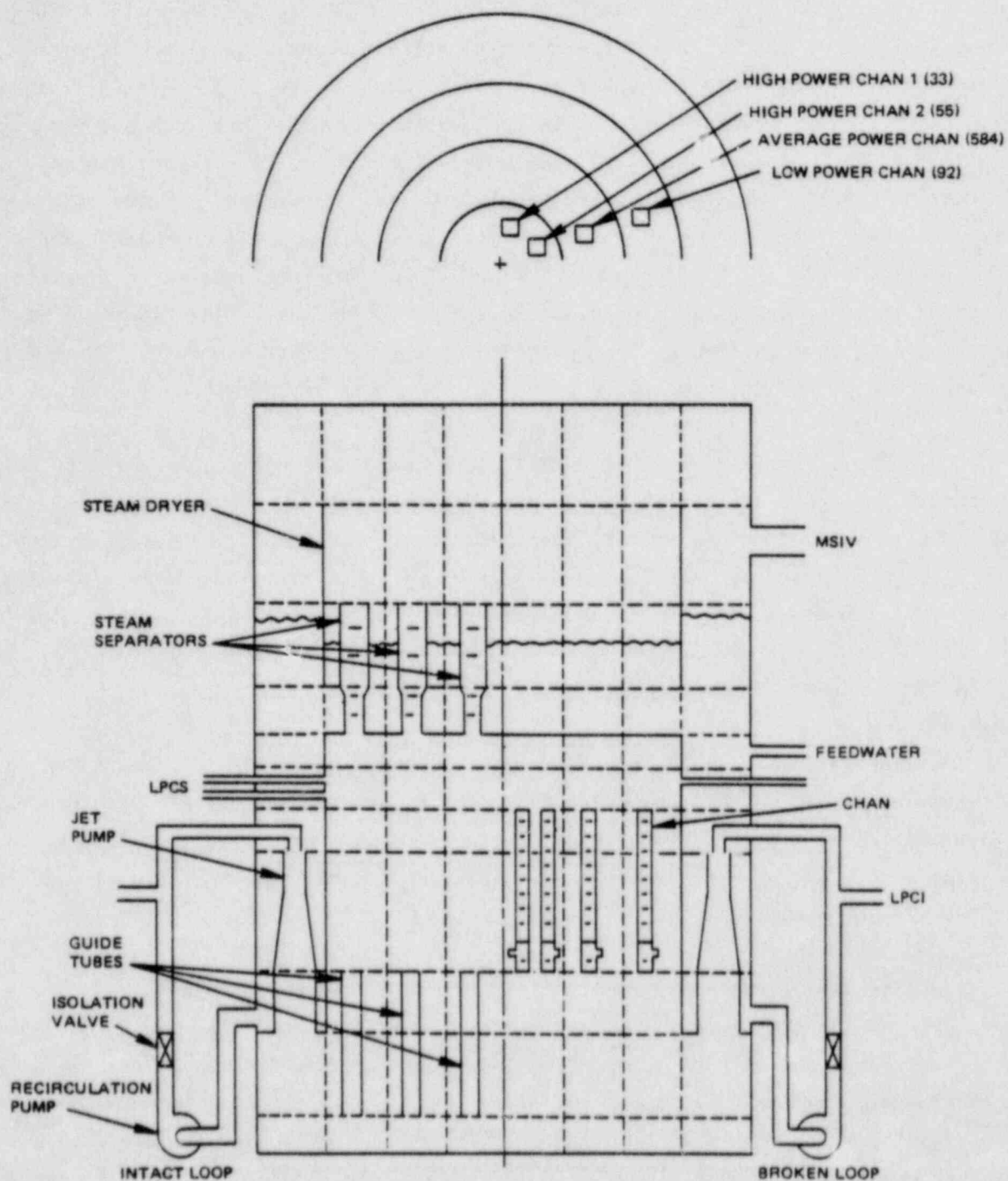


Figure 3-1. TRAC Nodalization BWR/4 Reactor Assembly

Three PIPE components, one in each of the three inner rings, are used to model the 185 guide tubes in a BWR/4-251 plant. These PIPE components represent 22, 146 and 17 guide tubes in Rings 1, 2 and 3, respectively. Similarly, three SEPARATOR components (one in each of the three inner rings) are used to model the 211 steam separators. The numbers of steam separators are 25, 161 and 25 in Ring #1, 2 and 3, respectively. The 2 recirculation loops are modeled by one broken loop and one intact loop in the TRAC calculation. Each loop consists of one suction PIPE component, one recirculation PUMP component, one LPCI isolative VALVE component, and one TEE component with the primary tube simulating the discharge pipe and the secondary tube connecting to a LPCI FILL component. The LPCI FILL component uses an appropriate pressure versus velocity table to simulate the LPCI flow rate. The discharge pipe of the recirculation loop connects to the drive line of the JETP component. Each JETP component simulates 10 jet pumps.

The ECCS lines are modeled by 3 PIPE components, each one is connected to a FILL component with appropriate pressure versus velocity table to simulate the LPCS flow rate. The other ends of these PIPE components are connected to the peripheral cell in the upper plenum, representing spray nozzles with different angle and elevation. The ECC spray sources and distributions are calculated by the upper plenum model (2).

3.3 RESULTS

Immediately following the break, the jet pump discharge flow in the broken loop reverses while the jet pump discharge flow in the intact loop initially increases and then slowly reduces with recirculation pump coast-down. As a result, the core flow is greatly reduced. The reduced core flow causes an early boiling transition in the high power fuel bundles.

The downcomer level drops rapidly as a result of the break flow. When this level drops below the break location a reduction in break mass flow and an increase in the depressurization rate occur. The increased depressurization causes the liquid in the lower plenum to flash and a temporary large upflow through the core and jet pumps results. The good heat transfer provided by this upflow completely quenches the fuel bundles. Following lower plenum flashing, the liquid drains out of the core and a heat up of the fuel occurs again. This heat up is more wide spread and observed for both the high and average power bundles.

When the pressure in the vessel is low enough, the LPCI comes on. The LPCI water is injected into the jet pump drive lines and through the jet pumps into the lower plenum. In the jet pumps a large amount of condensation occurs on the LPCI flow coming in through the nozzles. The condensation process is fed by steam entering the jet pump suction from the downcomer. As a result, the LPCI water is saturated as it leaves the jet pump discharge. This fills the lower plenum with a two-phase mixture, which subsequently floods into the core and quenches the second heatup in all bundles.

The sequence of important events of this calculation is summarized in Table 3-3. Reactor scram, recirculation pump trip and feedwater pump trip occurred immediately following the pipe break. The battery was assumed to have failed at time zero, which resulted in failure of the HPCI, 2 LPCIs and 1 LPCS. The MSIV trip also occurred at time zero. The MSIV has a delay time of 0.5 seconds and closure time of 5.0 seconds. It fully closed at 5.5 seconds into the transient.

Figure 3-2 shows the steam dome pressure for the BWR/4 DBA transient. The steam dome depressurized at a rate of 1.2 bars per second from 0.0 to 5.0 seconds. The steam dome pressure rose about 2 bars at 5.5 seconds due to the MSIV closure. After the suction pipe uncover at 7.6 seconds, the steam dome resumed depressurization at a rate of 1.4 bars per second.

The break flows from the broken suction pipe connected to the vessel and from the drive line in the broken loop are shown in Figures 3-3 and 3-4, respectively. The times of uncover for the drive line (5.0 seconds) and suction line (7.6 seconds) are indicated distinctly by the sudden reduction in break flows.

The LPCIs came on at 40.2 seconds and the LPCI isolation valves closed at 69.1 seconds. Before the isolation valves closed, the LPCI water injected into the broken loop drained down to the break location and became part of the break flow. At 1.5 seconds after the valves closed, the drive flow in the broken jet pump (Figure 3-4) changed to about 800 kg/s, which was the LPCI flow rate injected into the broken jet pump.

Table 3-3

SEQUENCE OF EVENTS FOR BWR/4 DBA RECIRCULATION BREAK

<u>Event</u>	<u>Time (sec)</u>
Recirculation line break	0.0
Power scram	0.0
Feedwater pump trip	0.0
Recirculation pump trip	0.0
Battery failure (HPCI, 2 LPCI, 1 LPCS)	0.0
MSIV closure started	0.5
Feedwater off	1.0
Jet pump drive uncover	5.0
MSIV fully closed	5.5
Recirculation suction line uncover	7.6
First boiling transition in PCT Node	8.6
Onset of lower plenum flashing	9.0
Second boiling transition in PCT node	31.0
LPCS on	38.5
LPCI on	40.2
LPCI Isolation valves closed	69.1
Second boiling transition quenched	81.0

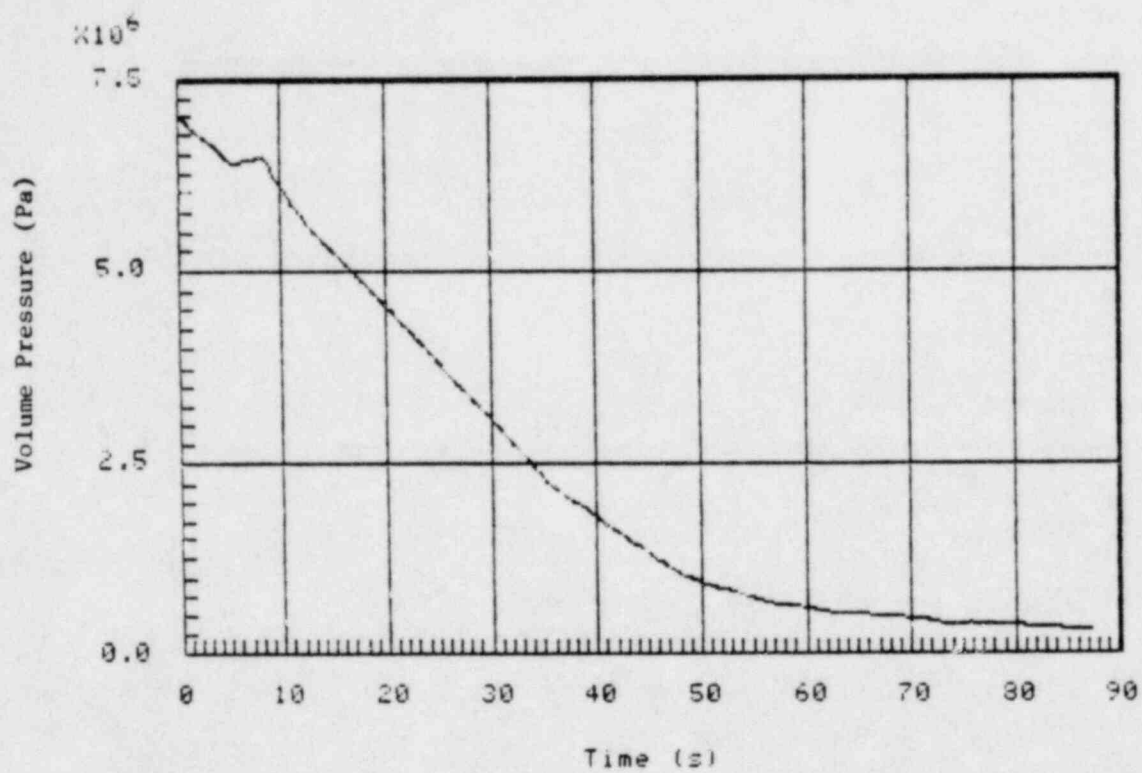


Figure 3-2. BWR/4 DBA Steam Dome Pressure

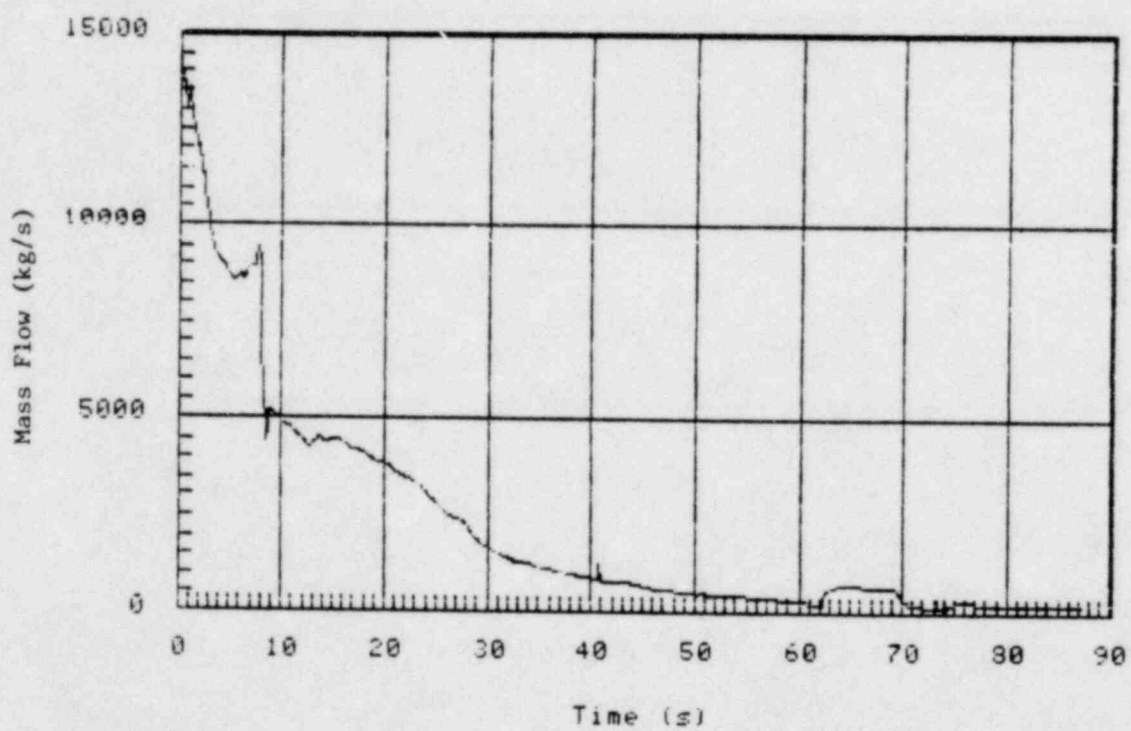


Figure 3-3. BWR/4 DBA Break Flow from Suction Line connected to Vessel

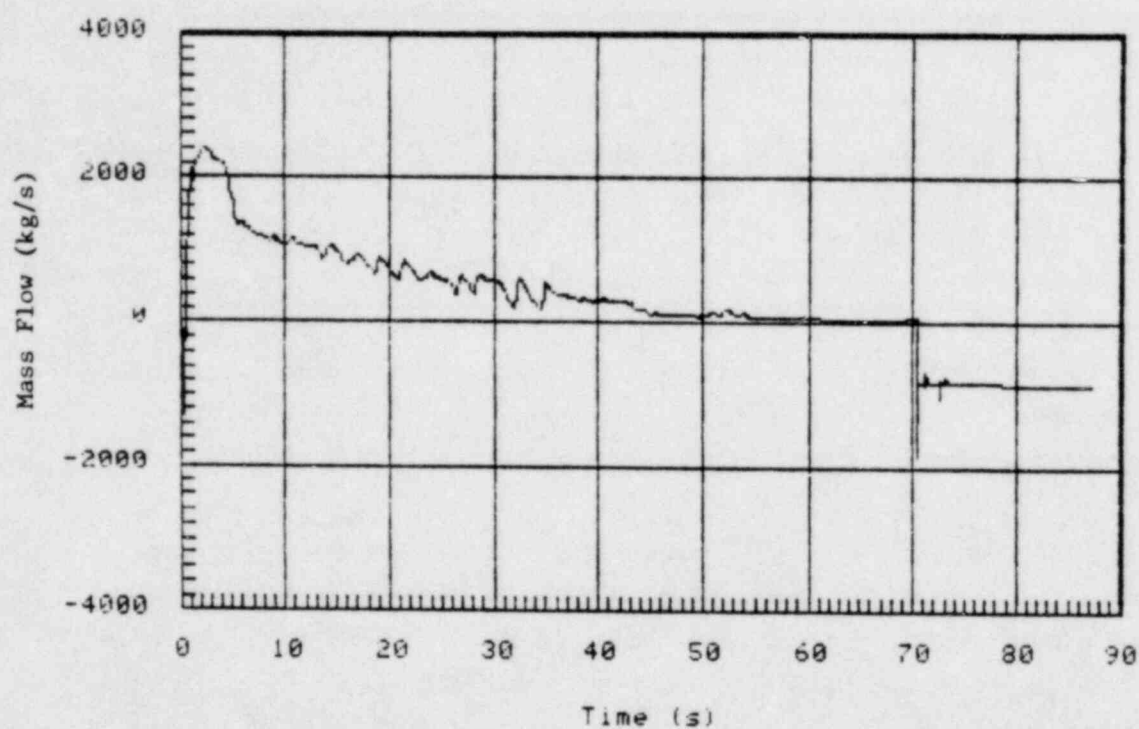


Figure 3-4. BWR/4 DBA Break Flow from Drive Line in Broken Loop
(Positive flow from drive line to break)

The jet pump discharge flow in the broken loop is shown in Figure 3-5. The discharge flow reversed at about 0.75 seconds following the pipe break and remained negative until 73 seconds. At 73 seconds (4 seconds after the isolation valves closed), the discharge flow changed to positive and remained constant for the rest of the calculation.

Figure 3-6 shows the jet pump discharge flow in the intact loop. The discharge flow initially increased and then slowly reduced as the recirculation pump coasted down. The LPCI water injected into the intact loop after 40 seconds and slowly filled up the lower portion of the loop. The loop became full at about 53 seconds. As a result, the discharge flow became positive after 53 seconds.

Figure 3-7 shows the mass inventories in the lower plenum and core normalized to the initial values. The onset of lower plenum flashing occurred at 9 seconds, which is clearly shown by the sudden drop of mass inventory in the lower plenum. The mass inventory in the lower plenum decreased monotonously until 53 seconds. At this time it reached the minimum value of 26% of the initial inventory. After 53 seconds, the mass inventory increased continuously due to the LPCI flow from the intact loop and reached 50% of the initial inventory at 73 seconds. After the LPCI isolation valves closed, the lower plenum refilling rate was about twice that before 73 seconds. At 87 seconds, the mass in the lower plenum had filled to about 75% of the initial inventory.

The mass inventory in the core showed a sudden rise in value at 9 seconds corresponding to the onset of lower plenum flashing. After that the core mass decreased monotonously and reached the minimum value of 6% initial inventory at 73 seconds. Shortly after the mass in the lower plenum had refilled to 50% of the initial inventory, two-phase mixture started flooding rapidly into the core. The core mass reached about 50% of the initial inventory at 80 seconds. After this time, the core was completely quenched by the reflooding two-phase mixture.

The refilling and reflooding process during a BWR/4 large break LOCA was previously simulated by system transient test in the Steam Sector Test Facility (SSTF) Reference 4). The test was conducted by initializing the mass distribution to that expected in the transient when the pressure reaches 150 psia (expected to be approximately 50 seconds after the LOCA) and then blowing the system down through a break. Figure 3-8 shows the regional mass of this system test. The lower plenum mass was

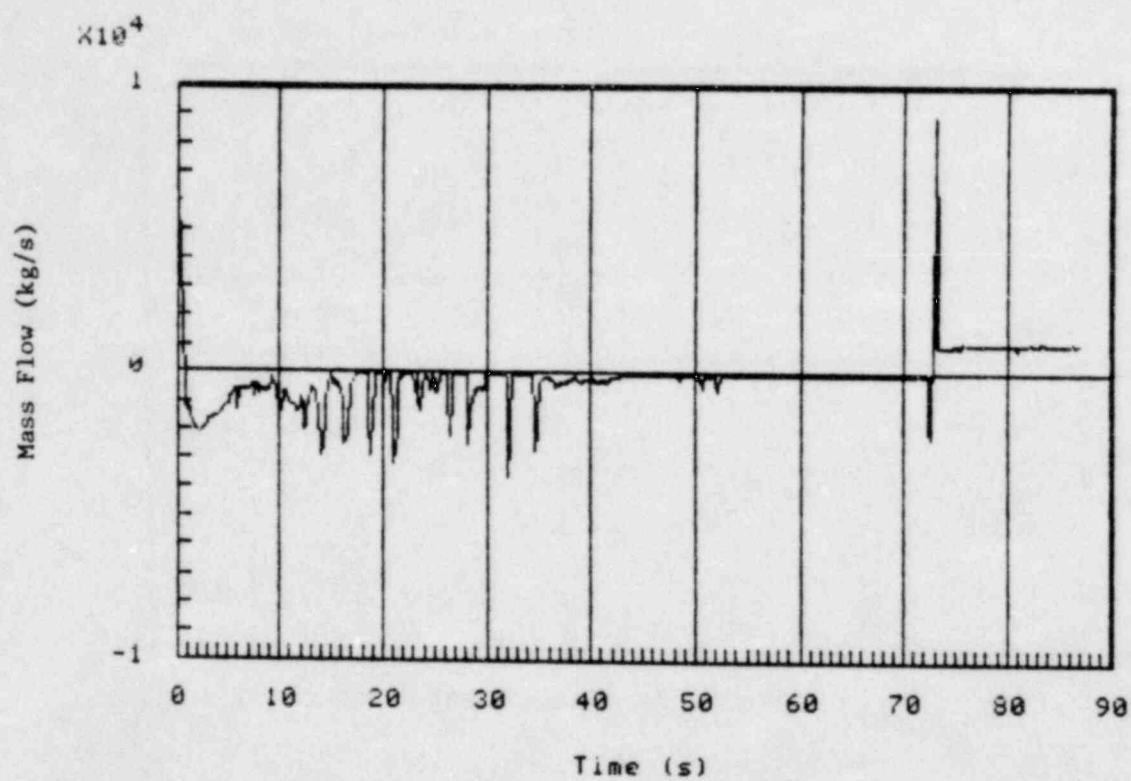


Figure 3-5. BWR/4 DBA Broken Jet Pump Discharge Flow

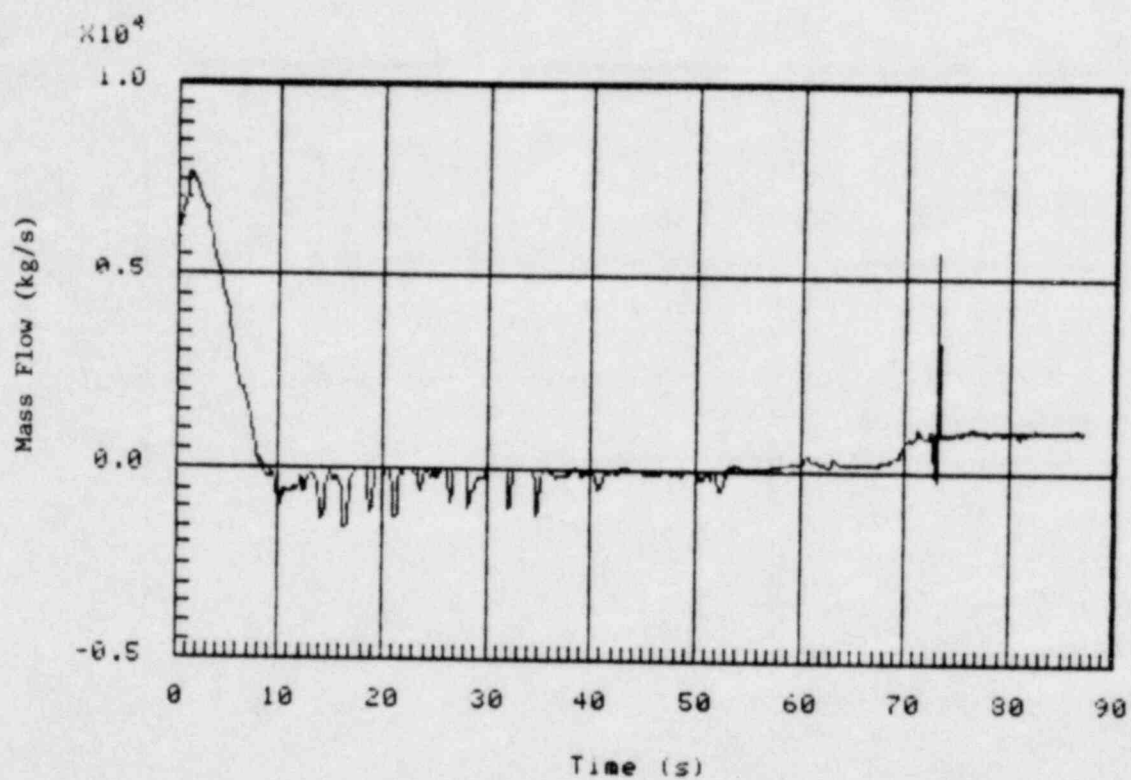


Figure 3-6. BWR/4 DBA Intact Jet pump Discharge Flow

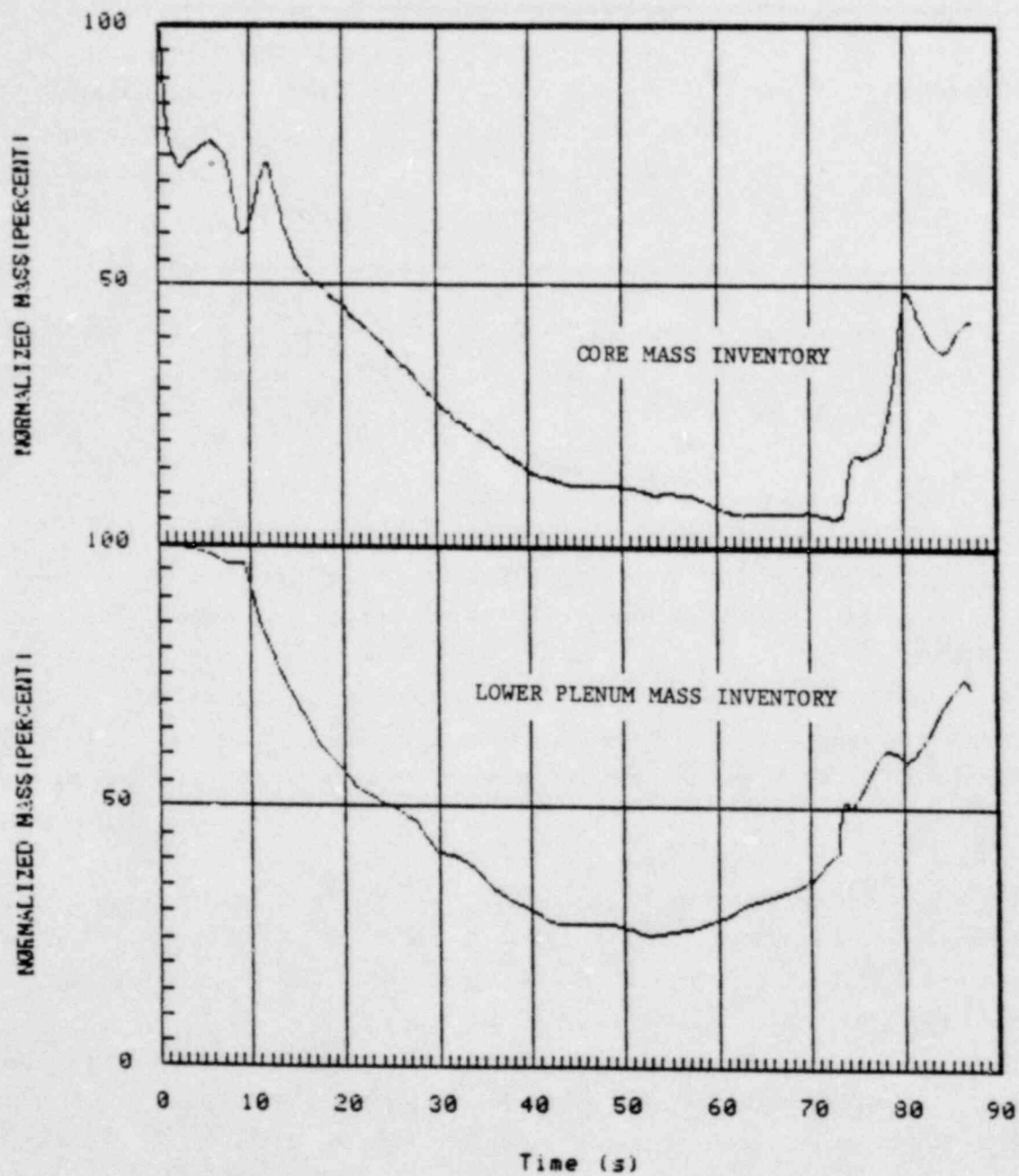


Figure 3-7. BWR/4 DBA Mass Inventories in Lower Plenum and Core Normalized to Initial Mass

initialized at 27% filled and reached 60% filled within 40 seconds from the start of the test. The core mass was initialized at 4% filled and showed a sudden rise when the lower plenum reached 40 % filled at 10 seconds after the start of the test. The core was filled to 50% within 25 seconds after the start of the test.

In this calculation, the system pressure (Figure 3-2) reached 150 psia at 48 seconds after LOCA. This timing compares very well with the test expected value of 50 seconds. One to one comparison between the test and calculation is not possible due to different geometry and initial conditions. However, by qualitatively comparing the last 40 seconds of the calculation (Figure 3-7) to the first 40 seconds of the test (Figure 3-8), it can be concluded that the calculated refilling and reflooding processes agree very well with those observed in the SSTF test.

Figures 3-9 through 3-16 show the mass flows at the bottom (side entry orifice) and at the top of bundle for Low Power CHAN, average Power CHAN, High Power CHAN #1 and High Power CHAN #2. These CHAN components simulate 92 peripheral bundles, 584 average power bundles, 33 and 55 high power bundles correspondingly.

For all types of bundles, the side entry orifice (SEO) flows (Figures 3-9, 3-11, 3-13 and 3-15) remained co-current upward until the suction line uncover (7.6 seconds). After the suction line uncover, more steam in the downcomer was allowed to escape from the break and the pressure in the downcomer region dropped faster than that in the lower plenum. As a result, the discharge flow of the intact jet pump reversed and all SEO flows became co-current downward. The core inventory drained down to the lower plenum during the time period from 7.6 seconds to about 9.0 seconds. At 9.0 seconds, the lower plenum started flashing, which caused the core flows to be upward again.

After the LPCI isolation valves closed at 69.1 seconds, both the intact and broken jet pump started filling up with LPCI water, i.e., started blocking off the lower plenum steam from escaping through the jet pumps. As a result, all SEO flows became upflow after 70 seconds.

Shortly after the lower plenum had refilled to 50% full by the LPCI flows, the core started reflooding from the lower plenum and the SEO flows of all types of bundles showed large positive upflow thereafter.

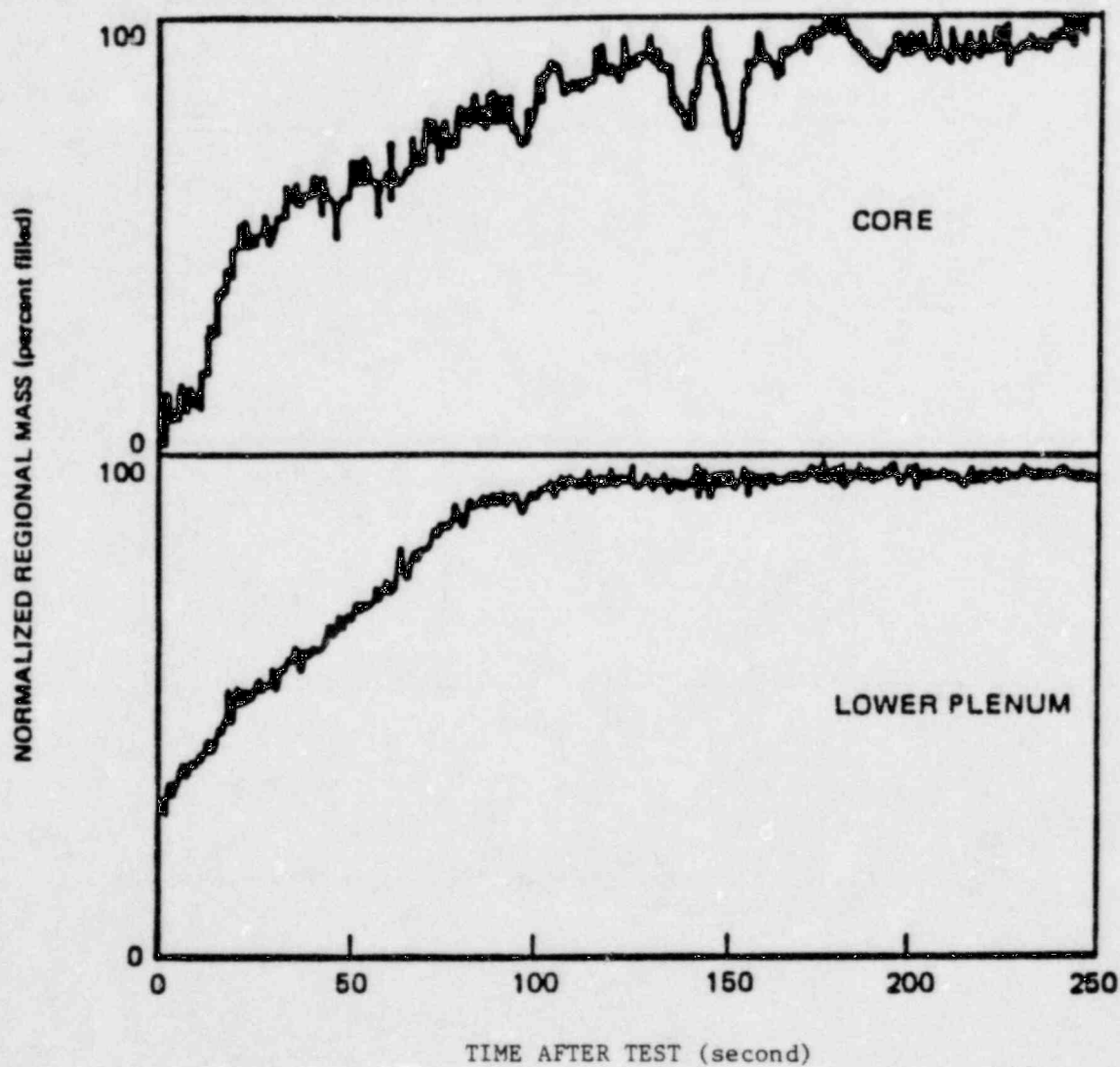


Figure 3-8. Regional Mass During SSTF BWR/4 Large Break LOCA Refill Test

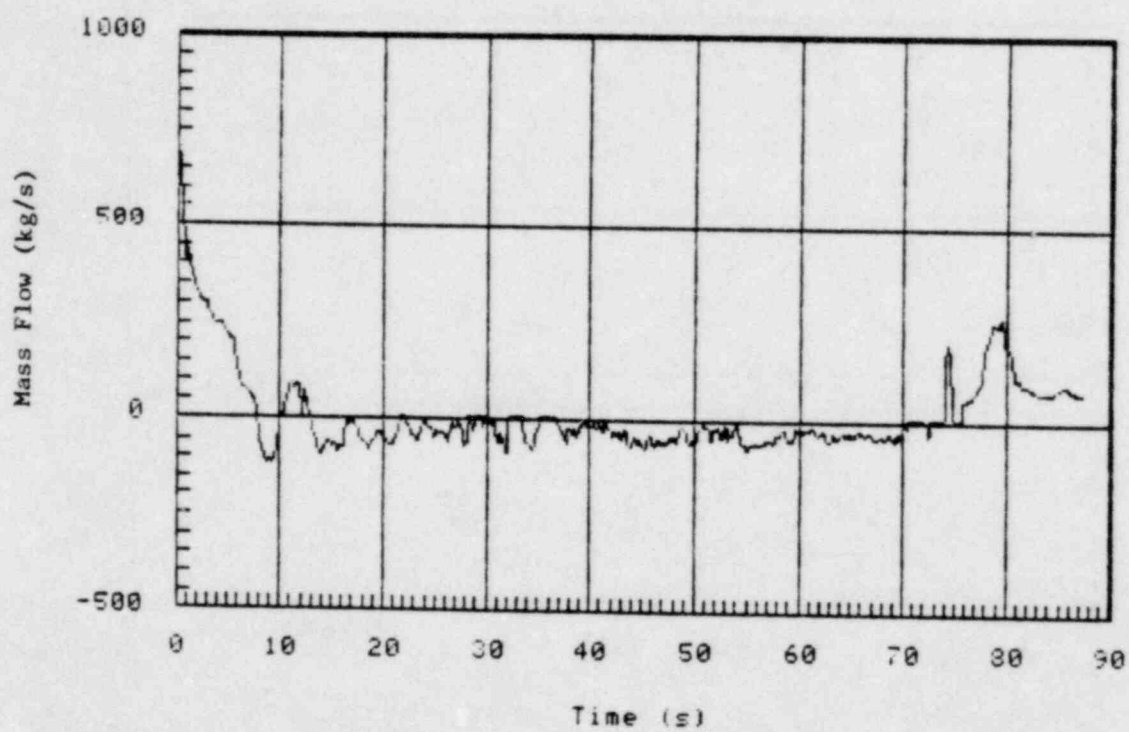


Figure 3-9. BWR/4 DBA Mass Flow at SEO of Low Power CHAN (92 Bundles)

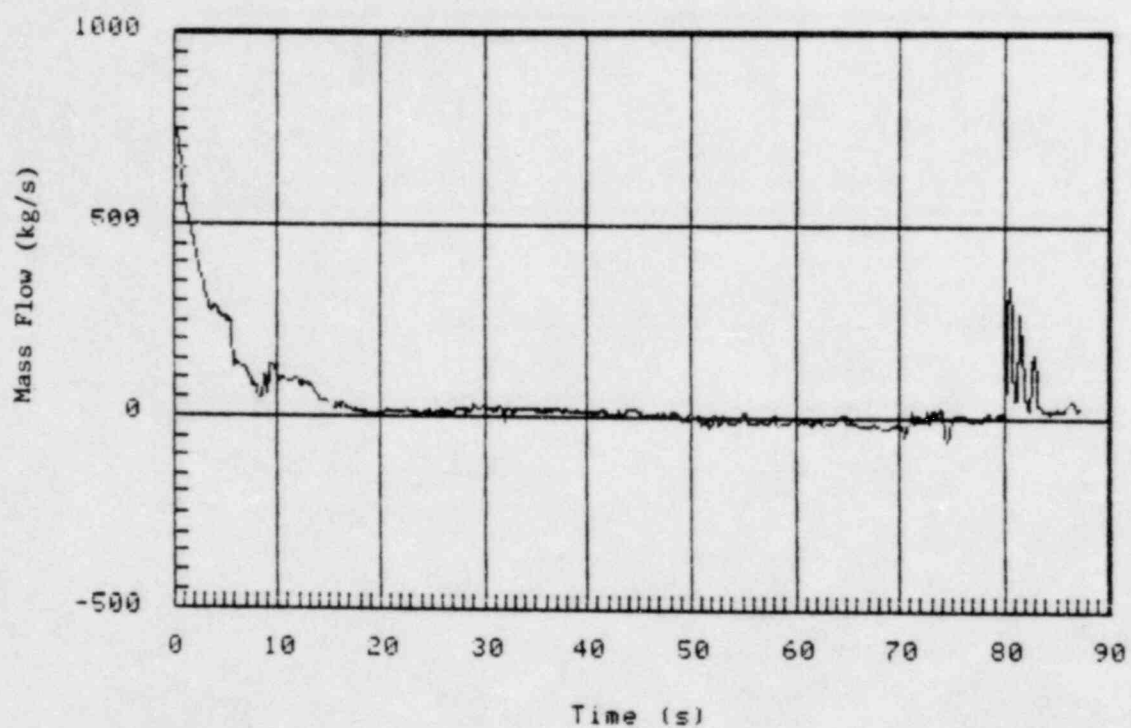


Figure 3-10. BWR/4 DBA Mass Flow at Top of Low Power CHAN
(92 Bundles)

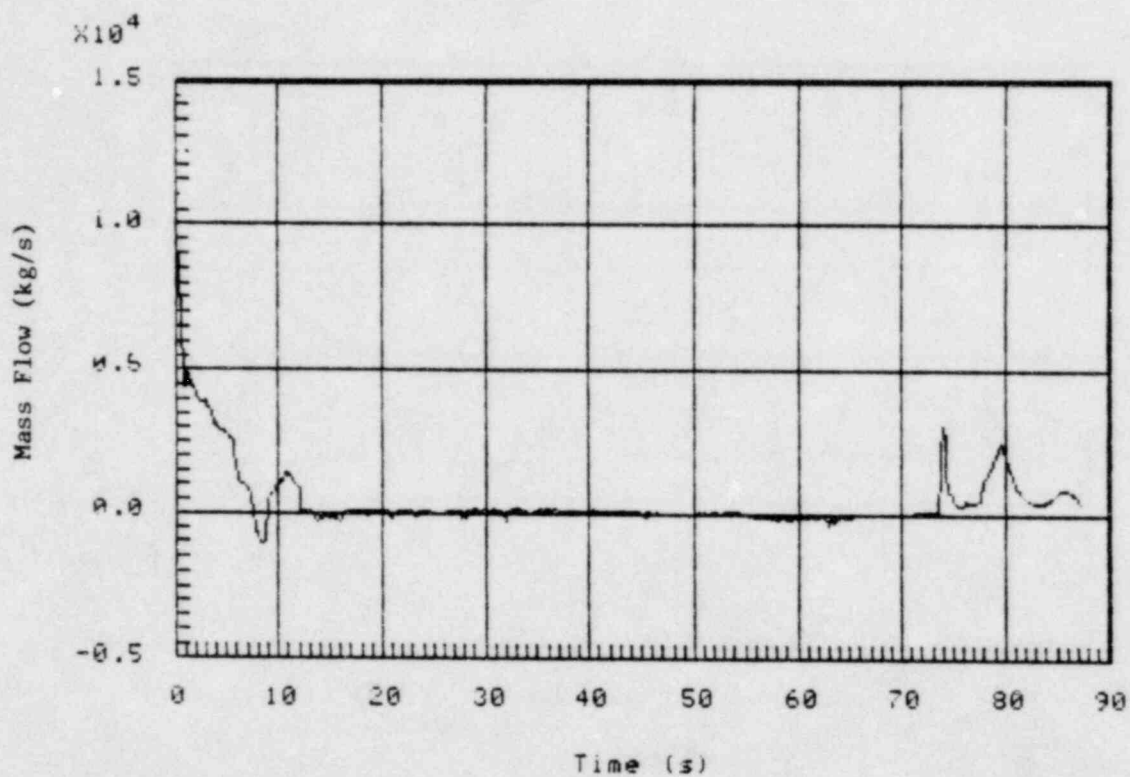


Figure 3-11. BWR/4 DBA Mass Flow at SEO of Average Power CHAN (584 Bundles)

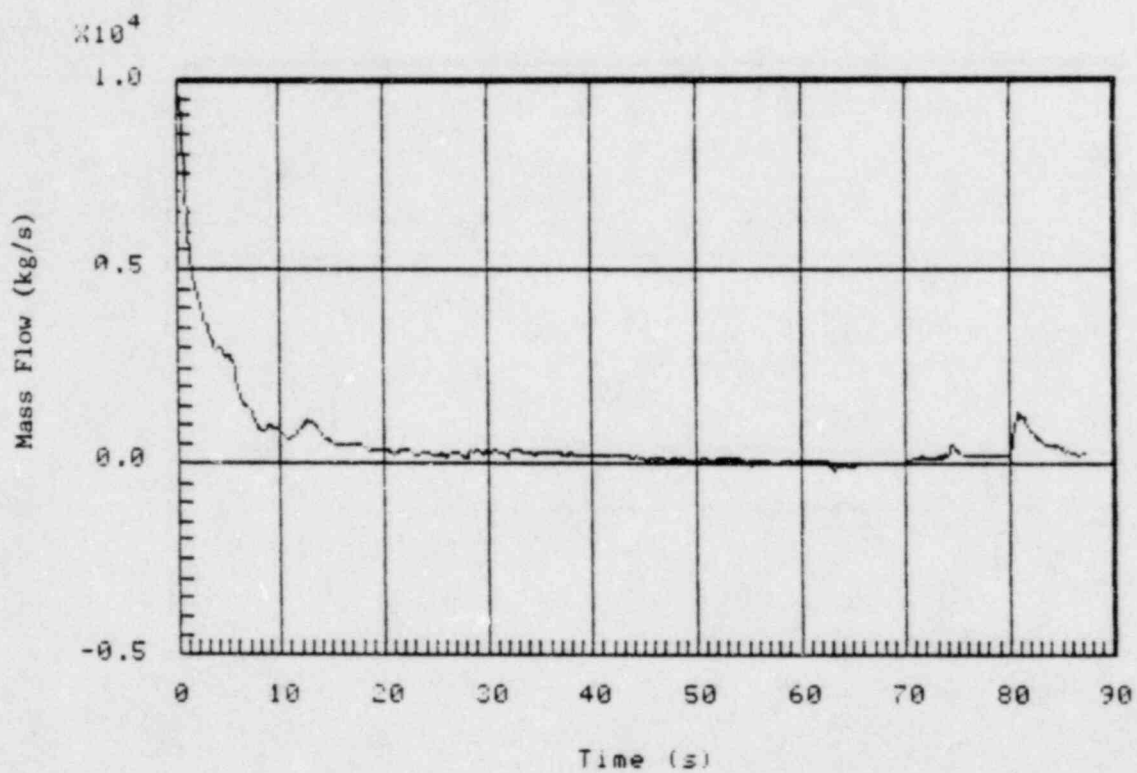


Figure 3-12. BWR/4 DBA Mass Flow at Top of Average Power CHAN
(584 Bundles)

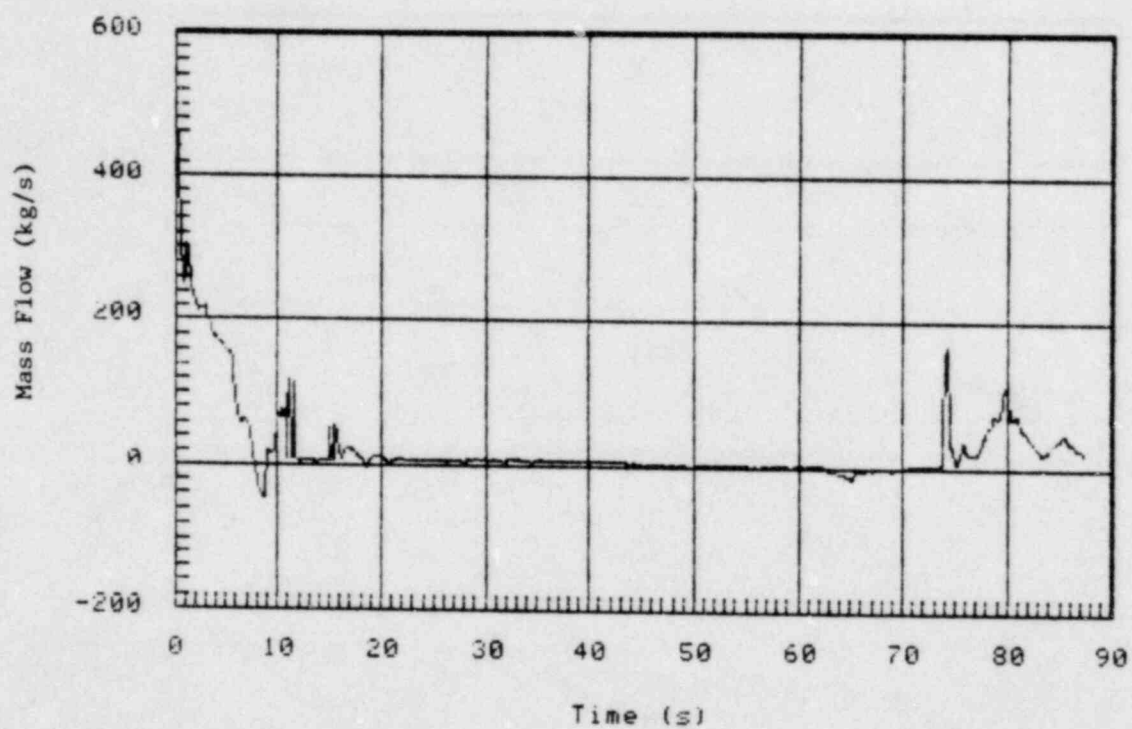


Figure 3-13. BWR/4 DBA Mass Flow at SEO of High Power CHAN #1 (33 Bundles)

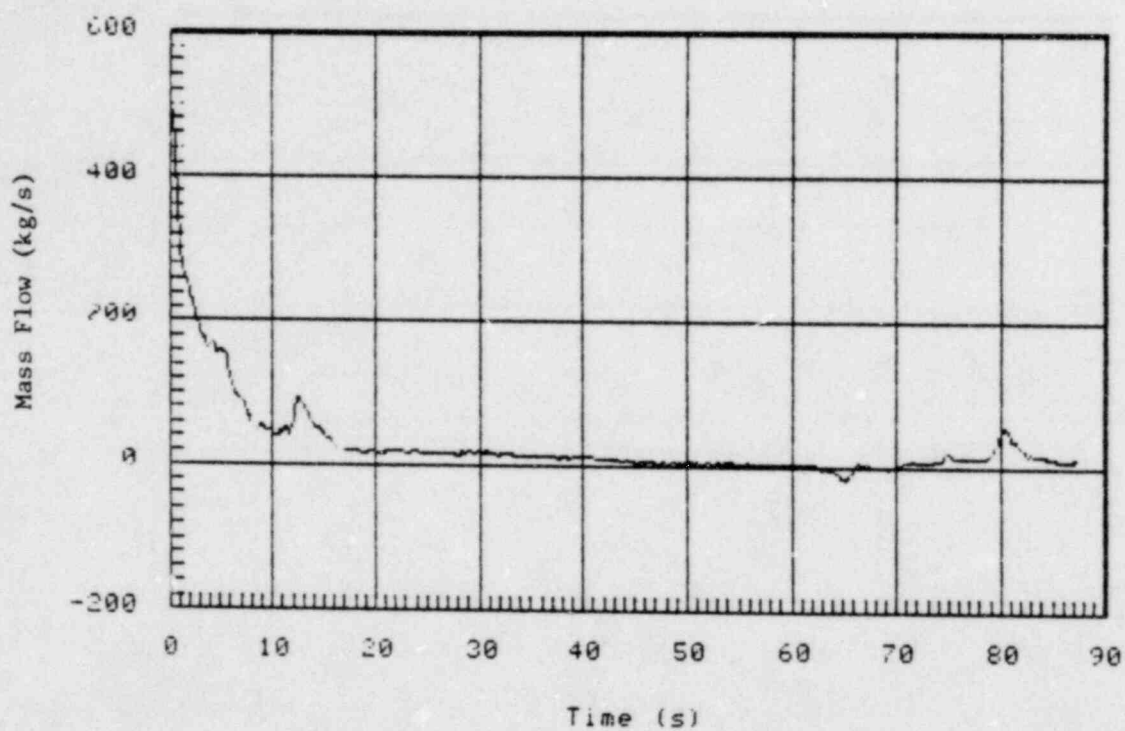


Figure 3-14. BWR/4 DBA Mass Flow at Top of High Power CHAN #1 (33 Bundles)

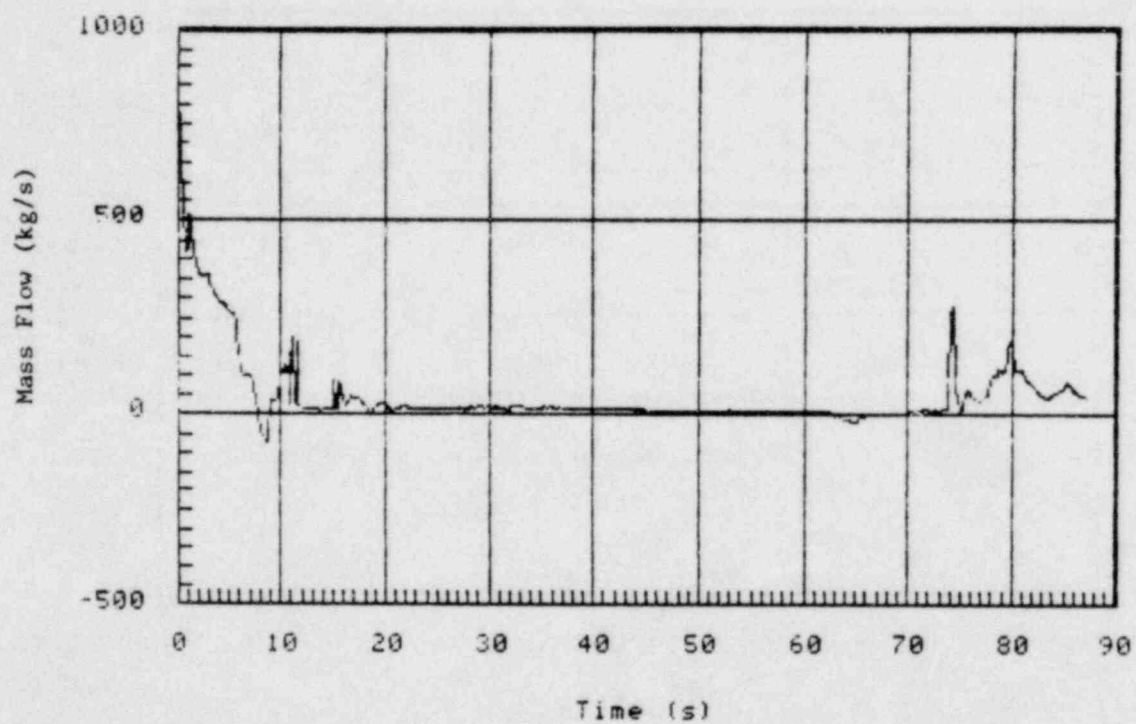


Figure 3-15. BWR/4 DBA Mass Flow at SEO of High Power CHAN #2
(55 Bundles)

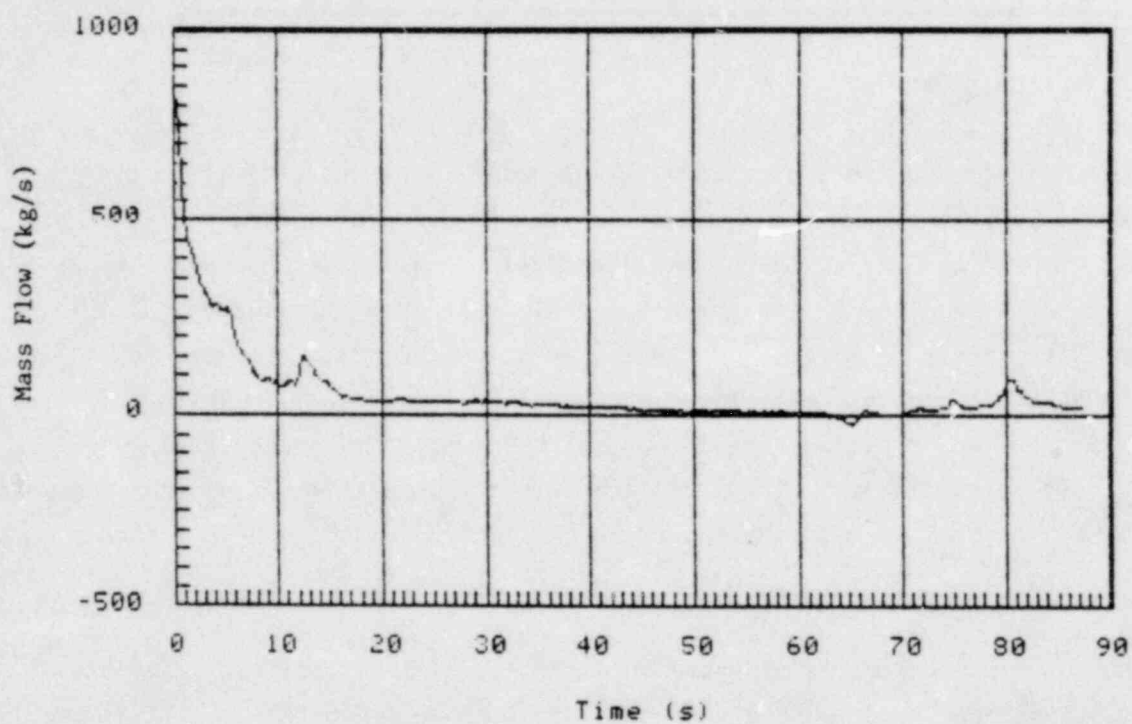


Figure 3-16. BWR/4 DBA Mass Flow at Top of High Power CHAN #2
(55 Bundles)

For the low power bundles, the top flow (Figure 3-10) was co-current upward until 15 seconds. After 15 seconds, the top flow was counter-current until the jet pumps were filled with LPCI water. For the average power bundles, the top flow (Figure 3-12) was co-current upward until 23 seconds, then it switched to counter-current until 70 seconds. For the high power bundles (Figures 3-14 and 3-16), the top flow was co-current upward until 40 seconds, then it changed to counter-current flow until 70 seconds. After 70 seconds, the top flows of all types of bundles changed to co-current upflow due to reflooding from the lower plenum.

Figure 3-17 shows the void fraction at the central cell in the upper plenum. After the LPCS came on at 38.5 seconds, the upper plenum started to accumulate liquid and formed a pool of two-phase mixture due to CCFL at the top of all bundles. However, no significant subcooling was observed at the top cell of any bundles for the whole transient calculation.

Figures 3-18 through 3-21 show the Peak Cladding Temperature (PCT) in the low power, average power and high power bundles. The PCT calculated by the High Power CHAN #1 and High Power CHAN #2 are almost identical in this case. As shown in Figure 3-18, the low power bundles did not have any heat up in this calculation. The average bundles (Figure 3-14) started heating up at 34 seconds. They reached a peak value of 550°K at 56 seconds. At this time the heat transfer by the ECC spray water down flow from the upper plenum turned over the temperature in the average bundle. The second heat up was about half cooled down by the ECC spray water at the time when the LPCI valves closed and was completely quenched at 79 seconds due to bottom flooding.

For the high power bundles (Figures 20 and 21), the first boiling transition started at 8.6 seconds, and reached a peak value of 630°K. The first boiling transition was quenched by the upward core flow induced by the onset of lower plenum flashing. The second boiling transition started at 31 seconds and reached a peak value of 620°K at 65 seconds. At this time the heat transfer by the ECC spray water downflow turned over the temperature in the high power bundles and held the temperature between 610 and 620°K until bottom flooding. The second heat up was completely quenched at 81 seconds due to bottom flooding.

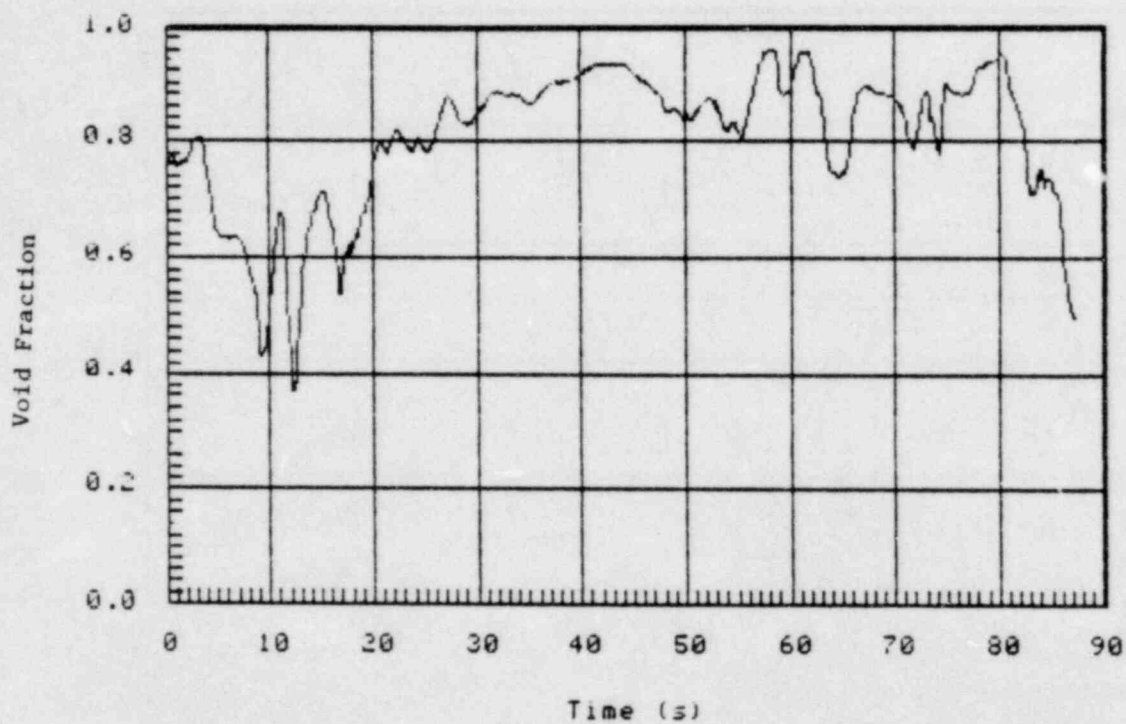


Figure 3-17. BWR/4 DBA Void Fraction at Central Cell in the Upper Plenum

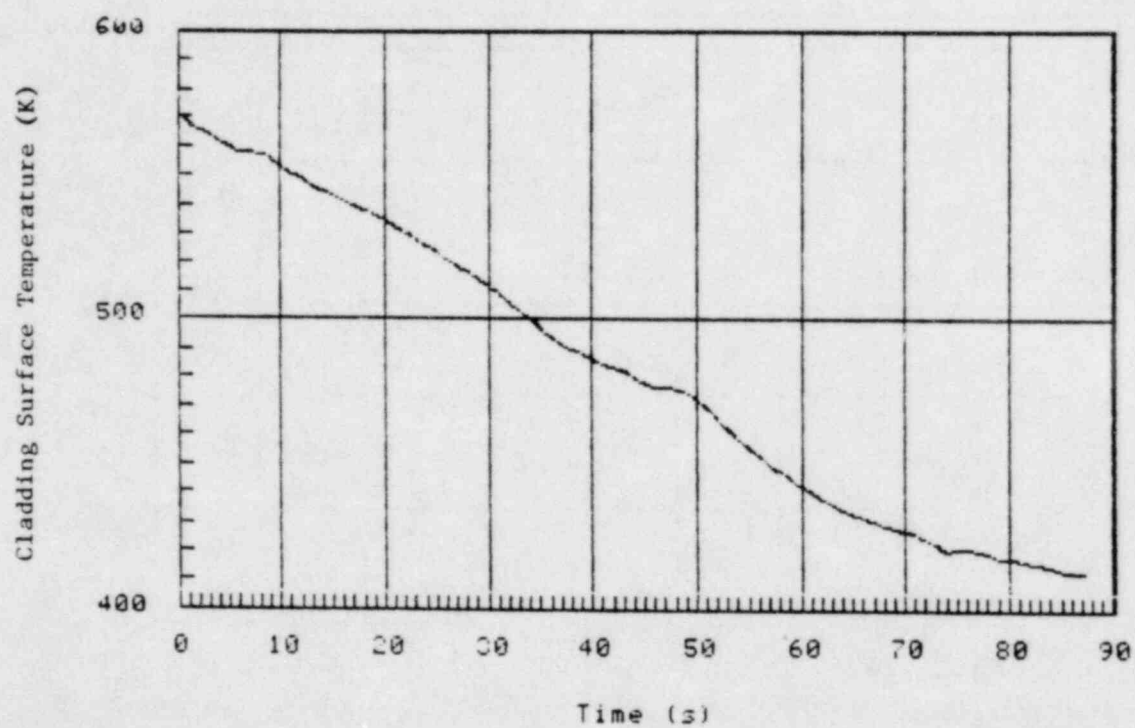


Figure 3-18. BWR/4 DBA Peak Cladding Temperature in Low Power Bundle

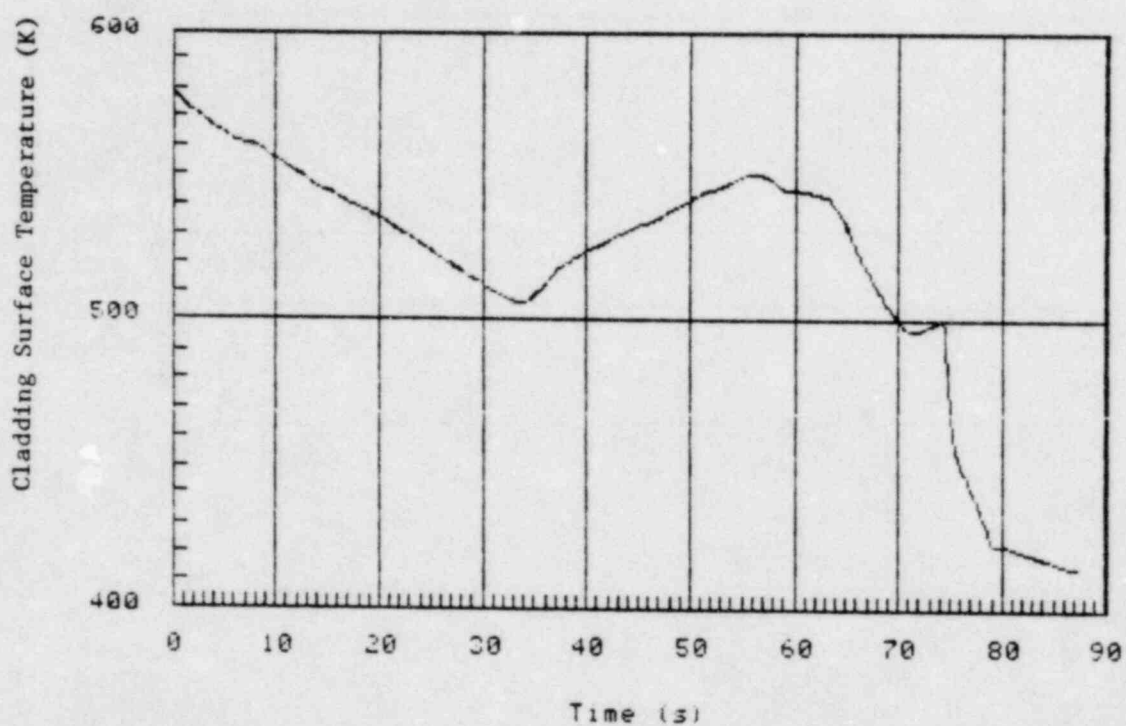


Figure 3-19. BWR/4 DBA Peak Cladding Temperature in Average Power Bundle

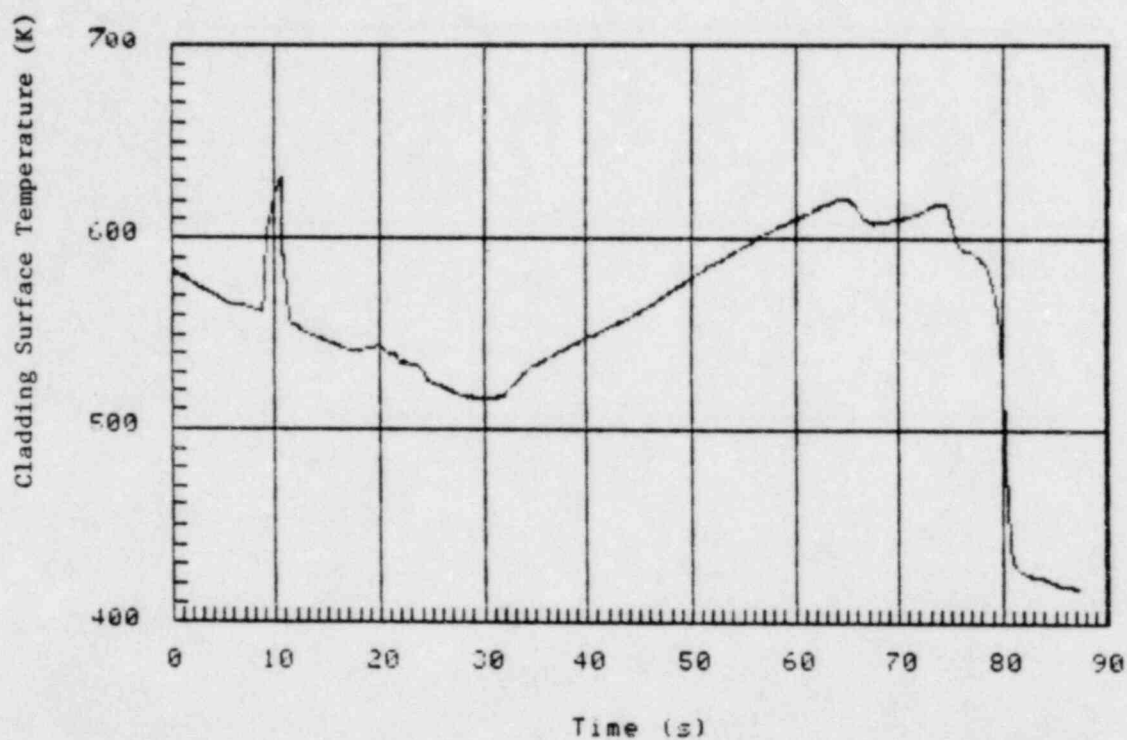


Figure 3-20. BWR/4 DBA Peak Cladding Temperature in High Power Bundle (CHAN #1)

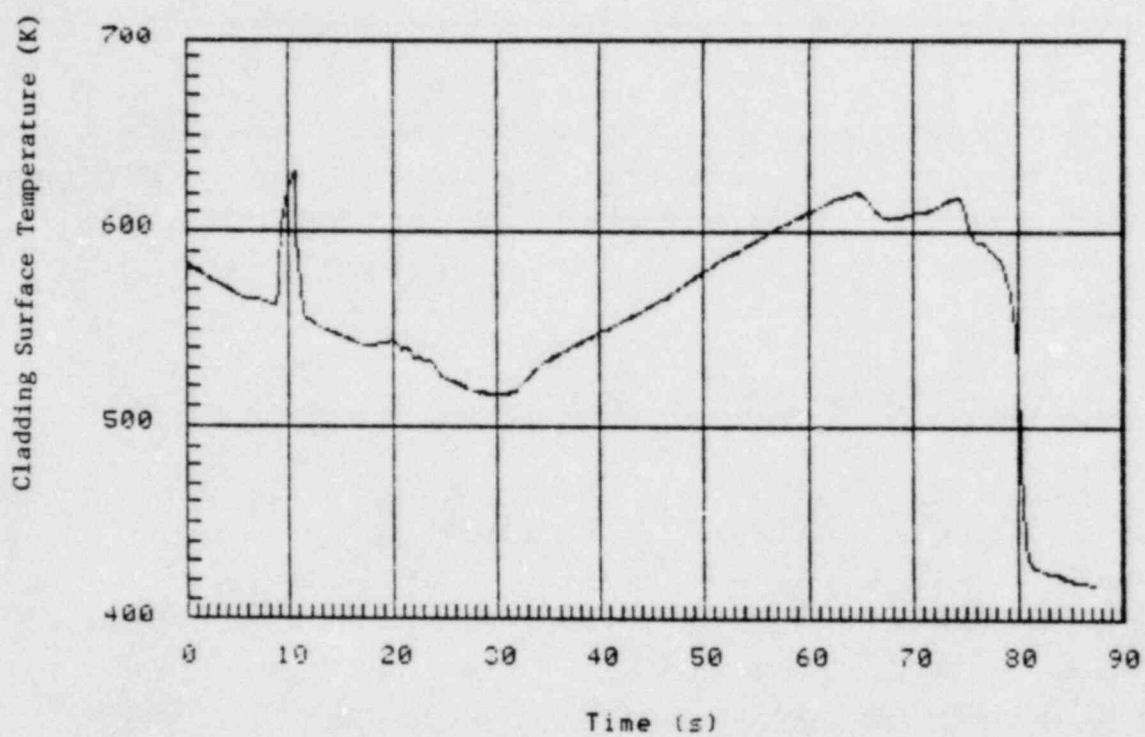


Figure 3-21. BWR/4 DBA Peak Cladding Temperature in High Power Bundle (CHAN #2)

3.4 MAIN OBSERVATIONS

From the BWR/4 DBA calculation a number of observations concerning the performance of the TRACB04 code and BWR/4 during a LOCA can be made:

TRACB04 performance

- o The overall performance of TRACB04 has been improved making it significantly easier to use than previous versions of the TRAC-BWR code. In particular, the improvements on the "water-packing" detection logic developed under the FIST program have been tested and the performance is very satisfactory.

BWR/4 LOCA characteristics

- o The ECC spray water from one LPCS forms a pool of two-phase mixture in the upper plenum due to CCFL at the top of all bundles. The liquid down flow from the upper plenum into the core produces sufficient heat transfer to turn over the second heat up and hold the hot spot at a low temperature level of 620°K until bottom flooding of the core.
- o The injection of LPCI water through the jet pumps into the lower plenum blocks off the lower plenum steam from escaping through the jet pumps. Furthermore, due to condensation on the LPCI water fed by steam from the downcomer, the LPCI water is saturated as it enters the lower plenum. Both of these features accelerate the entry of more two-phase mixture into the core. The core is flooded and completely quenched in 12 seconds after the LPCI isolation valves are closed. If the LPCI water were injected directly into the lower plenum, some of the above advantages would not be realized and the core reflooding and quenching would take relatively longer time to occur.
- o The maximum peak cladding temperature was 630°K and occurred shortly after the break.

SECTION 4

RUN-TIME STATISTICS

In general, the ratio of the Central Processor Unit (CPU) execution time to the real time depends on the size of the nodalization and phenomena involved in the calculation. The run-time statistics for the BWR/2 and BWR/4 DBA calculations with TRACB04 are listed in Table 4-1. For the DBA transients which included the blowdown, rod heatup and quenching, the run-time ratios are 119 and 126 for the BWR/2 and BWR/4 respectively. These ratios are about 4 and 6 times larger than those for the steady-state calculations.

Direct comparison of run-time statistics on BWR/2 and BWR/4 DBA transients with different versions of TRAC-BWR is not possible due to lack of data. However, the first ten seconds (blowdown phase) of a BWR/6 DBA transient has been performed using TRACB02, TRACB03 and TRACB04. This BWR/6 case was nodalized with 44 VESSEL cells and a total of 35 one-dimensional components. The size of this nodalization is compatible with those used in the BWR/2 and BWR/4 DBA calculations. Table 4-2 shows the summary of run-time statistics on the BWR/6 DBA case with TRACB02, TRACB03 and TRACB04. A comparison of the CPU to real time ratio on the steady-state case shows there is a factor of 21 improvement from TRACB02 to TRACB04. On the transient case, the improvement factors are 5.2 and 4.2 from TRACB02 and TRACB03 to TRACB04.

Table 4-1

Run-Time Statistics for the BWR/2 and BWR/4 DBA
Calculations with TRACB04

<u>Case</u>	<u>Problem time (sec.)</u>	<u>Ratio (= $\frac{\text{CPU time}}{\text{Real Time}}$)</u>
BWR/2 Steady-state	0.0 - 3.7	27.4
BWR/2 DBA Transient	0.0 - 201.1	119.3
<hr/>		
BWR/4 Steady-state	0.0 - 8.2	18.4
BWR/4 DBA Transient	0.0 - 87.2	125.6
<hr/>		

Table 4-2

Summary of Run-time Statistics on the BWR/6 DBA Calculations
with TRACB02, TRACB03 and TRACB04

<u>Case</u>	<u>Problem time (sec.)</u>	<u>Ratio (= $\frac{\text{CPU time}}{\text{Real Time}}$)</u>
BWR/6 Steady-state with TRACB02	0.0 - 1.00	301.1
BWR/6 Steady-state with TRACB03	-----	-----
BWR/6 steady-state with TRACB04	0.0 - 10.03	14.1
<hr/>		
BWR/6 DBA Transient with TRACB02	0.0 - 10.04	372.0
BWR/6 DBA Transient with TRACB03	0.0 - 10.04	300.4
BWR/6 DBA Transient with TRACB04	0.0 - 10.04	72.3
<hr/>		

SECTION 5

CONCLUSION

A BWR/2 and BWR/4 DBA has been performed to provide the best-estimate calculational data for these cases, and to assess the overall performance of TRACB04 in realistic plant simulations. In general, TRACB04 is more user-friendly, efficient and reliable than its predecessors. This is attributable to the implementation of the fast numerics, the improved Water-packing logic, and the time step control logic on the rate of change and rate of convergence on primitive variables.

The major conclusions from the BWR/2 DBA calculation are:

- (a) The containment model and air option implemented in TRACB04 work well and generate results in agreement with engineering judgement.
- (b) The containment response provides a beneficial feedback on the LOCA. The higher reactor vessel pressure helps the heat transfer process. The effect of the back flow of air into the vessel was to reduce the condensation in the upper plenum and retain subcooling in the ECC water. This enhances the spray heat transfer in the latter part of the transient.
- (c) The maximum PCT was quite low (1053°K) and occurred early in the transient.
- (d) The maximum drywell and wetwell pressures were 3.06 bars and 2.94 bars, respectively, well within the design limits.

The major conclusions from the BWR/4 DBA calculation are:

- (a) The maximum PCTs for both the first and second peak were very low (630°K and 620°K, respectively).
- (b) The hot spots in the core were completely quenched shortly after the LPCI isolation valves closed.

SECTION 6

REFERENCES

1. J.G.M. Andersen, K.H. Chu and J.C. Shaug, "BWR Refill-Reflood Program, Task 4.7- Model Development, Basic Models for BWR Version of TRAC", NUREG/CR-2573, EPRI NP-2375, GEAP-22051, September 1983.
2. Y.K. Cheung, V. Parameswaran and J.C. Shaug, "BWR Refill-Reflood Program, Task 4.7- Model Development, TRAC-BWR Component Models", NUREG/CR-2574, EPRI NP-2376, GEAP-22052, September 1983.
3. Md. Alamgir, "BWR Refill-Reflood Program, Task 4.8-TRAC-BWR Model Qualification for BWR Safety Analysis, Final Report", NUREG/CR-2571, EPRI NP-2377, GEAP-22049, October 1983.
4. L.L. Myers, "BWR Refill-Reflood Program, Final Report", NUREG/CR-3223, EPRI NP-3093, GEAP-30157, October 1983.

BIBLIOGRAPHIC DATA SHEET

SEE INSTRUCTIONS ON THE REVERSE

1. REPORT NUMBER (Assigned by TIDC, add Vol. No., if any)

NUREG/CR-4127, Vol. 3

EPRI NP-3987

GEAP-30875

2. TITLE AND SUBTITLE

BWR Full Integral Simulation Test (FIST) Program
TRAC BWR Model Development
Volume 3: Developmental Assessment for Plant Application

3. LEAVE BLANK

4. DATE REPORT COMPLETED

MONTH

YEAR

June

1985

6. DATE REPORT ISSUED

MONTH

YEAR

November

1985

5. AUTHOR(S)

Y.K. Cheung, J.G.M. Andersen, K.H. Chu, J.C. Shaug

7. PERFORMING ORGANIZATION NAME AND MAILING ADDRESS (Include Zip Code)

General Electric Company
Nuclear Technology and Fuel Division
175 Curtner Avenue
San Jose, CA 95125

8. PROJECT/TASK/WORK UNIT NUMBER

9. PIN OR GRANT NUMBER

B3014

10. SPONSORING ORGANIZATION NAME AND MAILING ADDRESS (Include Zip Code)

Division of Accident Evaluation
Office of Nuclear Regulatory Research
U.S. Nuclear Regulatory Commission
Washington, D.C. 20555

11a. TYPE OF REPORT

Technical

b. PERIOD COVERED (Inclusive dates)

12. SUPPLEMENTARY NOTES

13. ABSTRACT (200 words or less)

The TRACBC4 computer code has been developed under the model development tasks in the FIST Program. This report describes two developmental assessment calculations performed on BWR plants with TRACB04. A BWR/2 Design Basis Accident (DBA) including the containment response and a BWR/4 DBA with Low Pressure Coolant Injection (LPCI) water injected into the lower plenum were calculated and results of these cases were documented. These cases serve to test some of the new features of the TRACB04 (air field, containment model, "water packing" fixes and faster numerics in the three dimensional vessel component) and to demonstrate that the code has been assembled properly. They also provide best estimate LOCA results for the two plant types.

14. DOCUMENT ANALYSIS - a. KEYWORDS/DESCRIPTORS

Boiling Water Reactor (BWR)
Loss-of-Coolant Accident (LOCA)
Full Integral Simulation Test (FIST)
Transient Reactor Analysis Code (TRAC)

b. IDENTIFIERS/OPEN-ENDED TERMS

15. AVAILABILITY
STATEMENT

Unlimited

16. SECURITY CLASSIFICATION

(This page)

Unclassified

(This report)

Unclassified

17. NUMBER OF PAGES

18. PRICE

UNITED STATES
NUCLEAR REGULATORY COMMISSION
WASHINGTON, D.C. 20555

OFFICIAL BUSINESS
PENALTY FOR PRIVATE USE, \$300

FOURTH CLASS MAIL
POSTAGE & FEES PAID
USNRC
WASH D.C.
PERMIT No. G 87

RECEIVED BY THE NUCLEAR REGULATORY COMMISSION ON 11/11/87